SUPPLEMENTARY INFORMATION

An Isoindoline Bridged $[M(\eta^6\text{-arene})_2]^+$ (M = Re, ^{99m}Tc) *Ansa*-Arenophane and its Dinuclear Macrocycles with Axial Chirality

Joshua Csucker,[a] Da Kyung Jo,[a] Qaisar Nadeem,[a] Olivier Blacque,[a] Thomas Fox,[a] Henrik Braband[a] and Roger Alberto[a‡]

[a]Department of Chemistry, University of Zurich, Winterthurerstrasse 190, CH-8057 Zürich, Switzerland.

‡E-Mail: ariel@chem.uzh.ch

TABLE OF CONTENTS

1 Materials and Methods

1.1 Abbreviations

Abbreviation	Definition
arom.	aromatic
br	broad (NMR/IR)
C_q	quaternary carbon
d	doublet
dd	doubly distilled
DMF	dimethylformamide
Et	ethyl
GC	gas chromatogram
HPLC	High Performance Liquid Chromatography
HR-ESI-MS	high resolution electron spray ionization mass spectrometry
Napht	Naphthalene

Abbreviation	Definition
nd	not determined
NPhth	Phthalimide
OTf	Triflate
q	quadruplet
R_t	Retention time (HPLC/UPLC)
s	singlet
SDS	Sodium dodecane sulfate
t	triplet
TFA	trifluoroacetic acid
UPLC	Ultra-High-Performance Liquid Chromatography

1.2 General Methods and Materials

Hazards:

Caution: ^{99m}Tc is a γ-emitter. All experiments involving Tc chemistry must be carried out in licensed and appropriately shielded laboratories for low-level radioactive materials.

Materials & Methods:

Chemicals: Unless otherwise stated, all chemicals were of reagent grade or higher, obtained from commercial sources and used without further purification. **Solvents:** Solvents for reactions were of p.a. grade or distilled prior to their use; H_2O was bi-distilled. Deuterated NMR-solvents were purchased from *Armar Chemicals* or *Cambridge Isotope Laboratories, Inc.* (UK). **pH:** *Merck* indicator paper pH 1–14 (universal indicator). **General Technique:** When indicated, reactions were carried out under N_2 using standard *Schlenk* techniques in oven-dried (120 °C) glass equipment and monitored for completion by analyzing a small sample (after suitable workup) by UPLC or UPLC-ESI-MS. Evaporation of the solvents *in vacuo* was done with the rotary evaporator. **Radioactive materials:** Na[^{99m}TcO$_4$] in 0.9% saline was eluted from a ^{99}Mo/^{99m}Tc *Ultratechnekow FM* generator purchased from *Mallinckrodt Medical B.V.* (The Netherlands).

Instrumentation:

Microwave: Reactions were carried out in an *Anton Paar, Monowave 200* (Re-reactions) or a *Biotage Initiator* (^{99m}Tc-reactions) microwave.

NMR: ^{1}H- ^{13}C-NMR and 2D correlation spectra: *Bruker AV2-400* (400 MHz) or *Bruker AV2-500* (500 MHz); in deuterated solvents at 296 K (unless stated otherwise); chemical shifts (δ) in ppm relative to residual solvent resonances (CD_3CN ^{1}H: δ1.94, ^{13}C: δ1.32;); coupling constants (*J*) in Hz. Signal assignments are based on 2D-NMR experiments.

IR spectra: *SpectrumTwo FT-IR Spectrometer* (*Perkin–Elmer*) equipped with a *Specac Golden Gate™ ATR* (attenuated total reflection) accessory; applied as neat samples; $1/\lambda$ in cm^{-1}.

HR-ESI-MS: *QExactive* (*Thermo Fisher Scientific*, Bremen, Germany) equipped with a heated ESI source connected to a *Dionex Ultimate 3000* UPLC system. Samples dissolved in MeOH, MeOH/CH_2Cl_2 3:1, MeOH/H_2O 1:1, DMSO/H_2O 1:10, or H_2O at ca. 50 µg mL^{-1}; injection of 1 µL on-flow with an XRS auto-sampler (*CTC*, Zwingen, Switzerland)(mobile phase: MeOH + 0.1% HCOOH or CH_3CN/H_2O (2:8) + 0.1% HCOOH; flow rate 120 µL mL^{-1}); ion source parameters: spray voltage 3.0 kV, capillary temperature 280 °C, sheath gas 30 L min^{-1}, s-lens RF level 55.0; aux gas temperature 250 °C; full scan MS in alternating (+)/(−)-ESI mode; mass ranges 80–1'200, 133–2'000, or 200–3'000 amu; resolution (full width half-maximum) 70'000; automatic gain control (AGC) target 3.00 10^6; maximum allowed ion transfer time (IT) 30 ms; mass calibration <2 ppm accuracy for *m/z* 130.06619–1621.96509 in (+)-ESI with *Pierce®* ESI calibration solutions (*Thermo Fisher Scientific*, Rockford, USA); lock masses: ubiquitous erucamide (*m/z* 338.34174, (+)-ESI). Indicated m/z values correspond to the most abundant monoisotopic mass with the associated characteristic Re isotopic pattern(s).

UPLC-ESI-MS: *Waters Acquity* UPLC System coupled to a *Bruker Daltonics HCT™* ESI-MS, using an *Acquity UPLC BEH* C18 1.7 µm (2.1 x 50 mm) column. UPLC solvents were formic acid (0.1% in millipore water) (solvent A) and acetonitrile UPLC grade (solvent B). Applied UPLC gradient: 0–0.5 min: 95% A, 5% B; 0.5–4.0 min: linear gradient from 95% A, 5% B to 0% A, 100% B; 4.0–5.0 min: 0% A, 100% B. The flow rate was 0.6 mL min^{-1}. Detection was performed at 250 and 480 nm (DAD). Indicated m/z values correspond to the most abundant monoisotopic mass with the associated characteristic Re isotopic pattern(s).

Analytical UPLC: *VWR HITACHI Chromaster Ultra* system, using an *Acquity UPLC BEH* C18 1.7 µm (2.1 x 50 mm) column. UPLC solvents were trifluoroacetic acid (0.1 % in millipore water) (solvent A) and acetonitrile UPLC grade (solvent B). Applied UPLC gradient: 0–0.5 min: 95% A, 5% B; 0.5–4 min: linear gradient from 95% A, 5% B to 0% A, 100% B; 4–5 min: 0% A, 100% B. The flow rate was 0.5 mL min^{-1}. Detection was performed at 250 and 480 nm (DAD).

Preparative HPLC: *Shimadzu Prominence Modular HPLC* system, comprised of a *CBM-40* controller module, *SPD-40* cell unit, *LC-20AP* binary pump module and a *FCV-200AL* quaternary valve, using a *Dr. Maisch Reprosil* C18 100-7 (40 x 250 mm) column. HPLC solvents were *dd*H_2O (0.1 vol% trifluoroacetic acid buffer) (solvent A) and HPLC grade acetonitrile (solvent B). The flow rate was 40 mL/min. Analyte detection was performed at indicated wavelengths.

HPLC analyses of ^{99m}Tc complexes: *Merck Hitachi Chromaster 5160* pump coupled to a *Merck Hitachi Chromaster 5430* diode array detector and a radiodetector. UV-Vis detection was performed at indicated wavelenghts. The detection of radioactive ^{99m}Tc complexes was performed with a *Berthold FlowStar LB 514* radiodetector equipped with a *BGO-X* cell. Separations were achieved on a *Macherey-Nagel NUCLEOSIL®* C18 5 µm, 100 Å (250 × 3 mm) column. HPLC solvents were *dd*H_2O (0.1 vol% trifluoroacetic acid buffer) (solvent A) and HPLC grade acetonitrile (solvent B). The flow rate was 0.5 mL/min.

X-ray diffractometer:

X-ray diffraction: Single-crystal X-ray diffraction data collections for **[3][PF$_6$]** and **[5][PF$_6$]** were obtained on a Rigaku Oxford Diffraction XtaLAB Synergy, Dualflex, Pilatus 200K diffractometer while the single-crystal X-ray diffraction data collections for **[6a][TFA]$_2$** and **[6b][TFA]$_2$** were obtained on a Rigaku Oxford Diffraction SuperNova/Atlas area-detector diffractometer. All measurements were carried at 160(1) K using the Cu Ka radiation (l = 1.54184 Å) from a micro-focus X-ray source and an Oxford Instruments Cryojet XL cooler. The selected suitable crystals were mounted using polybutene oil on a flexible loop fixed on a goniometer head and transferred to the diffractometer. Pre-experiments, data collections, data reductions and analytical absorption corrections[1] were performed with the program suite *CrysAlisPro*.[2] Using *Olex2*,[3] the structures were solved with the *SHELXT*[4] small molecule structure solution program and refined with the *SHELXL 2018/3* program package[5] by full-matrix least-squares minimization on F^2. *PLATON*[6] was used to check the result of the X-ray analyses. The crystal data collections and structure refinement parameters are summarized in Chapter 2.4. CCDC 2142820 for **[3][PF$_6$]**, 2142821 for **[5][PF$_6$]**, 2142822 for **[6b][TFA]$_2$** and 2142823 for **[6a][TFA]$_2$** contain the supplementary crystallographic data for these compounds, and can be obtained free of charge from the Cambridge Crystallographic Data Centre via www.ccdc.cam.ac.uk/data_request/cif. The crystal structure of **[3][PF$_6$]** was refined as a two-component non-merohedral twin [scale: 0.1760(5) / 0.8240(5)]. The minor component was rotated by 180° around [0 1 0] in the reciprocal space or around [0.17 0.97 0.20] in the direct space.

1.3 Synthesis

[Re(η^6-C$_6$H$_6$)$_2$][OTf]

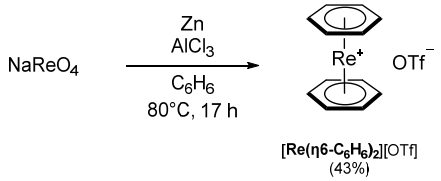

Procedure adapted from literature.[7] $NaOReO_4$ (1.00 g, 3.66 mmol, 1.0 eq), Zn powder (0.72 g, 11.00 mmol, 3.0 eq) and $AlCl_3$ (4.55 g, 36.00 mmol, 10.0 eq) were added to a 100 mL two necked Schlenk round bottom flask equipped with a reflux condenser under N_2 atmosphere. Benzene (50 mL) were added. The resulting black reaction mixture was stirred at 80 °C for 17 h. The residual solvent was removed *in vacuo*. Addition of H_2O (50 mL) at room temperature to the crude reaction mixture

caused intense fuming. The aqueous mixture was washed with Et_2O (4 × 50 mL). To the aq. phase was added LiOTf (0.69 g, 4.1 mmol, 1.1 eq). The aq. phase was purified by continuous liquid to liquid extraction with CH_2Cl_2 to provide the title compound [**Re(η^6-C$_6$H$_6$)$_2$**][OTf] (0.78 g, 1.6 mmol, 43 %) as bright yellow powder. The anionic counterion may be altered by addition of $NaPF_6$ or NH_4PF_6 to the aq. phase instead of LiOTf before performing the liquid to liquid extraction.

Data of [**Re(η^6-C$_6$H$_6$)$_2$**][OTf]:

^{1}H NMR (CD_3CN, 400 MHz): δ (ppm) = 5.94 (*s*, 6 arom. CH). **^{13}C NMR** (CD_3CN, 100 MHz): δ (ppm) = 77.1 (*s*, 6 arom. CH). **UPLC-ESI-MS**: R_t = 0.5 min, $[M]^+$ = calc.: 343.05 m/z, found: 343.03 m/z. (Analytical data agreed with literature values[7])

[**1**][PF_6]

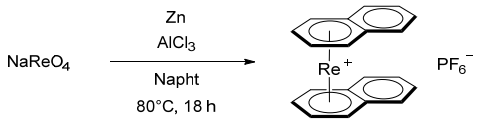

[**1**][PF_6] (27%)

$NaReO_4$ (1.00 g, 3.7 mmol, 1.0 eq), Zn powder (726 mg, 11.0 mmol, 3.0 eq), excess naphthalene (11.0 g), and anhydrous $AlCl_3$ (9.0 g, 37 mmol, 10 eq) were mixed in a Schlenk flask (100 mL) under N_2 and the suspension was heated at 100°C for 18 h. The reaction flask was protected from light. The black sticky crude reaction mixture was cooled to r.t. and dissolved in 1 M HCl (200 mL, at 0°C) and CH_2Cl_2 (500 mL) and filtered through glass filter frit into 2 L flask. Dissolution was increased by sonication for 1-2 min. The filter cake was suspended in 1 M HCl (50 mL × 5) and CH_2Cl_2 (2 × 50 mL) and filtered. The combined aqueous and DCM filtrate was sonicated for 1-2 min heated to 50°C and filtered again. The resulting reddish aqueous phase containing product was decanted. The organic layer was extracted with *dd*H_2O (4 × 100 mL). The aqueous phase was washed with CH_2Cl_2 (2 × 200 mL) and Et_2O (200 mL). NH_4PF_6 (1.0 g, 6.1 mmol, 1.65 eq) was added to the aqueous phase and the title compound was extracted with CH_2Cl_2 (3 × 150 mL). The solvent of the combined organic layer was removed *in vacuo*. [**1**][PF_6] (570 mg, 0.97 mmol, 27%) was obtained as a red powder.

Data of [**1**][PF_6]:

^{1}H NMR (CD_3CN, 400 MHz): δ (ppm) = 7.43-7.41 (*dd* like *m*, 4 arom. CH); 6.83-6.81 (*dd* like *m*, 4 arom. CH); 6.64-6.62 (*dd* like *m*, 4 arom. CH); 6.21-6.20 (*dd* like *m*, 4 arom. CH). **^{13}C NMR** (CD_3CN, 100 MHz): δ (ppm) = 129.4 (2 arom. CH); 128.9 (2 arom. CH); 89.7 (1 arom. C_q); 77.4 (2 arom. CH); 72.7 (2 arom. CH). **UPLC-ESI-MS**: R_t = 1.7 min, $[M]^+$ = calc.: 443.08 m/z, found: 443.06 m/z. (Analytical data agreed with literature values[8])

Synthesis of [**2a**][PF_6] and [**2b**][PF_6]:

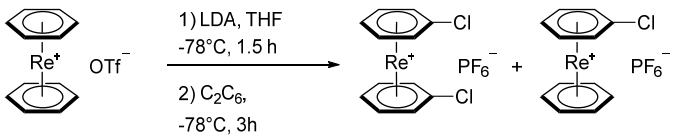

[**1**][OTf] [**2a**][PF_6] (31%) [**2b**][PF_6] (25 %)

Procedure adapted from literature.[9] **[Re(η^6-C$_6$H$_6$)$_2$]**[OTf] (200 mg, 407 µmol, 1.0 eq) and dry THF (20 mL) were added to a *Schlenk* round bottom flask (100 mL) under nitrogen. The resulting yellow suspension was cooled to -78 °C using an acetone/dry ice bath, and LDA (1.0 M, 1 mL, 1 mmol, 2.5 eq)

was added dropwise. Upon the addition of LDA, there was an immediate color change from yellow to orange, and over time, the color turned brown. After 1.5 h, hexachloroethane (385 mg, 1.6 mmol, 4.0 eq) was added, resulting in a color change from brown to light orange. The reaction was continued to be stirred for 3 h at -78 °C. The reaction was quenched with 0.1 vol % aq. TFA (1 mL) and solvent was removed under reduced pressure. The crude was dissolved in 0.1 vol % aq. TFA (1 mL) and CH_3CN (3 mL) and purified on preparative HPLC (R_t =19.1 min ([**2a**]$^+$), Rt =24.3 min ([**2b**]$^+$),hold 10% B for 5 min, 10 to 30% B in 35 min, 30 to 100% B in 5 min, hold 100% B for 5 min/268 nm). The fractions containing the desired products were lyophilized. Counterion exchange was carried out by dissolving each product in water then adding it to saturated aq. NH_3PF_6. The resulting precipitates were collected by filtration or centrifugation to give compounds [**2a**][PF_6] (71 mg, 128 µmol, 31%) and [**2b**][PF_6] (54 mg, 103 µmol, 25%) as yellow solids.

Data of [**2a**][PF_6]:

^{1}H NMR (CD_3CN, 400 MHz): δ (ppm) = 6.50 (*d*, J = 5.9 Hz, 4 arom. CH, *o*-CH_{arom}); 6.12 (*t*, J = 5.7 Hz, 4 arom. CH, *m*-CH_{arom}); 5.90 (*t*, J = 5.4, 2 arom. CH, *p*-CH_{arom}). **^{13}C NMR** (CD_3CN, 100 MHz): δ (ppm) = 101.6 (C_q, 2 C, C-Cl); 82.2 (4 arom. CH, *o*-CH_{arom}); 79.4 (2 arom. CH, *p*-CH_{arom}); 78.6 (4 arom. C, *m*-CH_{arom}). **UPLC-ESI-MS**: R_t = 1.2 min, [M]$^+$ = calc.: 410.97 m/z, found: 410.98 m/z. (Analytical data agreed with literature values[9])

Data of [**2b**][PF_6]:

^{1}H NMR (CD_3CN, 400 MHz): δ (ppm) = 6.51 (*d*, J = 5.8 Hz, 2 arom. CH, *o*-CH_{arom}); 6.04 (*t*, J = 5.6 Hz, 2 arom. CH, *m*-CH_{arom}); 6.02 (*s*, 6 arom. CH, CH_{arom}); 5.84 (*t*, J = 5.3, 1 arom. CH, *p*-CH_{arom}). **^{13}C NMR** (CD_3CN, 100 MHz): δ (ppm) = 100.0 (C_q, 1 C, C-Cl); 80.7 (6 C, CH_{arom}); 79.7 (2 arom. CH, *o*-CH_{arom}); 76.9 (1 arom. CH, *p*-CH_{arom}); 75.7 (2 arom. CH, *m*-CH_{arom}). **UPLC-ESI-MS**: R_t = 0.7 min, [M]$^+$ = calc.: 377.01 m/z, found: 377.00 m/z. (Analytical data agreed with literature values[9])

Synthesis of **[3]**[TFA]:

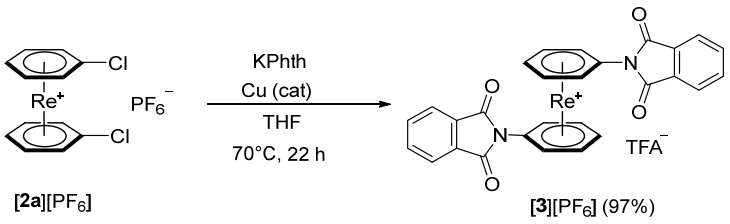

A *Schlenk* round bottom flask (50 mL) was charged with [**2a**][PF_6] (30 mg, 53.9 µmol, 1.0 eq), potassium phthalimide (50 mg, 269.7 µmol, 5.0 eq) and dry THF (10 mL) under nitrogen, and the reaction mixture was refluxed at 70 °C for 22 h. After cooling the reaction mixture to r.t., the suspension was filtered and solvent was removed under reduced pressure. The crude was dissolved in 0.1 vol % aq. TFA (1 mL) and CH_3CN (3 mL) then purified on preparative HPLC (R_t = 26.5 min, hold 20% B for 5 min, 20% to 80% CH_3CN in 30 min, 80% to 100% B in 5 min, hold 100% B for 5 min/268 nm). The title compound [**3**][TFA] (39 mg, 52.2 µmol, 97%) was obtained as a yellow solid. Counterion exchange was carried out by dissolving the compound in CH_2Cl_2 (5 mL), adding H_2O (5 mL) and saturated aq. NH_3PF_6, then collecting the organic phase. The solvent was removed under reduced pressure, giving [**3**][PF_6] as a yellow solid.

Data of [**3**][TFA]:

^{1}H NMR (CD_3CN, 400 MHz): δ (ppm) = 7.80-7.73 (sym. *m*, 8 arom. CH, CH_{arom}); 6.57 (*d*, J = 6.1 Hz, 4 arom. CH, *o*-CH_{arom}); 6.21 (*t*, J = 5.7, 4 arom. CH, *m*-CH_{arom}); 5.98 (*t*, J = 5.3 Hz, 2 arom. CH, *p*-CH_{arom}). **^{13}C NMR** (CD_3CN, 100 MHz): δ (ppm) = 167.4 (C_q, 4 C, C=O); 136.3 (C_q, 4 C); 131.9 (4 C, CH_{arom}); 124.5 (4 C, CH_{arom}); 96.4 (C_q, 2 C); 77.83 (2 C, *p*-CH_{arom}); 77.77 (4 C, *o*-CH_{arom}); 77.6 (4 C, *m*-CH_{arom}). **FT-IR** (neat) ν [cm^{-1}]: 3434, 3169, 1729 (C=O), 1664, 1651, 1581, 1556, 1381, 1306, 1052, 837, 715. **HR-ESI-MS**: $C_{28}H_{18}N_2O_4Re$; $[M]^+$; calc.: 633.08186 m/z, found: 633.08149 m/z (-0.58 Δ ppm). **UV/Vis** (CH_2Cl_2):λ_{max} 281 nm 1.07×10^5 $M^{-1}cm^{-1}$. **Elemental Analysis:** [**3**][PF_6] ($C_{28}H_{18}F_6N_2O_4PRe$) calc.: 43.25% C; 2.33% H; 3.60 % N; found: 44.00% C; 2.20% H; 3.95% N.

Synthesis of [**4**][PF_6]:

Method A

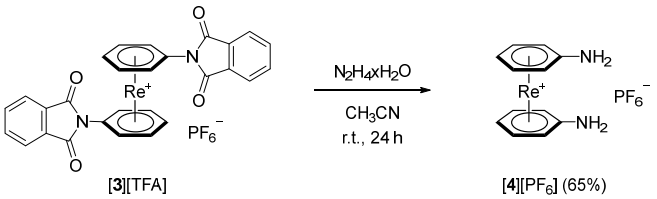

[**3**][TFA] (30 mg, 40 µmol, 1.0 eq) and CH_3CN (5 mL) were added to a round bottom flask (25 mL). Hydrazine hydrate (10 µL, 200 µmol, 5.0 eq) was added and the reaction was stirred at r.t. for 24 h. Solvent was removed *in vacuo*, and the crude was dissolved in 0.1 vol % aq. TFA (1 mL) and CH_3CN (3 mL) then purified on preparative HPLC (R_t =15.6 min, hold 10% B for 3 min, 10% to 100% B in 25 min, hold 100% B for 10 min/275 nm). Fractions containing the target material were collected and lyophilized. A yellow powder was obtained and dissolved in H_2O (5 mL). Addition of sat. aq. NH_4PF_4 resulted in precipitation of [**4**][PF_6] which was collected by centrifugation. The title compound [**4**][PF_6] (13 mg, 25 µmol, 65%) was obtained as a yellow solid.

Method B

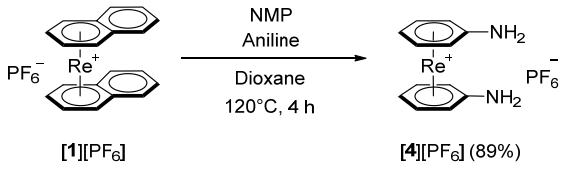

Adapted from a literature procedure.[10] Two batches of [$Re(Naph)_2$]PF_6 (30 mg, 112 µmol, 1.0 eq) were suspended in dry 1,4-dioxane (2 mL each) at r.t. in two separate *Schlenk* flasks equipped with a reflux condenser. *N*-methylprolidone (NMP. 25 µL each, 570 µmol, 5.0 eq) and aniline (1 mL each) were added to the reaction mixtures. The resulting red solutions were stirred at 120°C for 4 h during which time the solution changed color to dark brown. The crude reaction mixture was cooled to room temperature and concentrated under a N_2 stream. The two batches were combined and diluted with Et_2O (5 mL). The resulting brown suspension was extracted with aq. 0.1vol% TFA (5x1 mL). The aqueous layer was collected and purified by preparative HPLC (same method as Method A). Fractions containing the target material were collected and lyophilized. A yellow powder was obtained and dissolved in H_2O (5 mL). Addition of sat. aq. NH_4PF_4 resulted in precipitation of [**4**][PF_6] which was

collected by centrifugation. The title compound [**4**][PF_6] (47 mg, 91 µmol, 89 %) was obtained as a yellow powder.

Data of [**4**][PF_6]:

^{1}H NMR (CD_3CN, 400 MHz): δ (ppm) = 5.64 (*d*, J = 5.8 Hz, 4 H, *o*-CH_{arom}); 5.58 (*t*, J = 5.5 Hz, 4 H, *m*-CH_{arom}); 5.38 (*t*, J = 5.1, 2 H, *p*-CH_{arom}). **^{13}C NMR** (CD_3CN, 100 MHz): δ (ppm) = 77.2 (2 C, *p*-CH_{arom}); 73.4 (4 C, *o*-CH_{arom}); 63.8 (4 C, *m*-CH_{arom}). **HR-ESI-MS**: $[M]^+$ = calc.: 373.07090 m/z, found: 373.07034 m/z (1.52 Δ ppm). **Elemental Analysis:** [**4**][PF_6] ($C_{12}H_{14}F_6N_2PRe$) calc.: 27.86% C; 2.73% H; 5.41% N. found: 28.31% C; 2.76% H; 5.52% N. (Analytical data agreed with literature values[11])

Synthesis of [**5**][TFA], [**6a**][$TFA]_2$ and **[6b]**[$TFA]_2$:

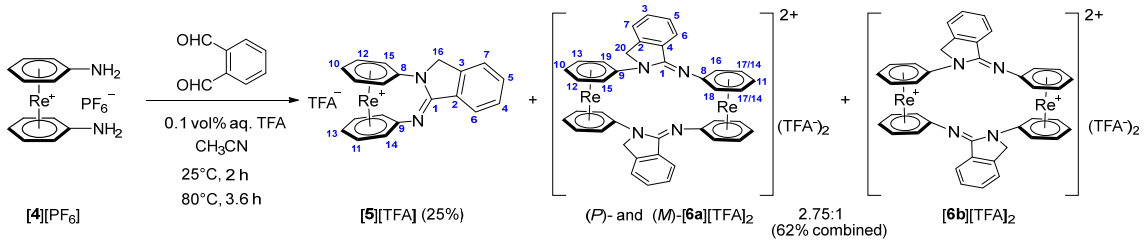

[**5**][PF_6] (36.0 mg, 70 µmol, 1.0 eq) was dissolved in CH_3CN (12 mL) and 0.1 vol% aq. TFA (1 mL) in a three necked round bottom flask (50 mL) equipped with two rubber septa and a N_2 inlet. *O*-Phthalaldehyde (10.3 mg, 77 µmol, 1.1 eq) was dissolved in CH_3CN (200 µL) in a separate vial, and the solution was taken into a *Hamilton* syringe. The aldehyde solution was slowly added to the reaction flask at 25°C using a syringe pump over 2 h with the flow rate of 100 µL/h. Upon complete addition of the aldehyde, the yellow reaction solution was heated to 80°C for 3.6 h after which time complete consumption of the [**5**][PF_6] was observed. The crude reaction mixture was cooled to r.t. and concentrated to a volume of 5 mL under a stream of N_2 and directly purified *via* preparative HPLC (R_t = 17.7 min ([**5**]$^+$), R_t = 24.0 min ([**6a**]$^{2+}$ and [**6b**]$^{2+}$); hold 20% CH_3CN for 5 min, 20 to 50% CH_3CN in 35 min, 50 to 100% CH_3CN in 5 min/240 nm). Fractions containing the title compounds were lyophilized to provide [**5**][TFA] (9.8 mg, 17 µmol, 25%) and a mixture of [**6a**][$TFA]_2$ and [**6b**][$TFA]_2$ in a ratio of 2.75:1 according to ^{1}H NMR (combined: 24.5 mg, 22 µmol, 62%) as light yellow solids. Counterion exchange was carried out by dissolving [**5**][TFA] in CH_2Cl_2 (5 mL), adding H_2O (5 mL) and saturated aq. NH_3PF_6, then collecting the organic phase. The solvent was dried over $MgSO_4$ and removed *in vacuo*. [**5**][PF_6] was obtained as a yellow solid. An analytically pure sample of [**6a**][$TFA]_2$ was obtained by crystallization *via* vapor diffusion of Et_2O into a CH_3CN solution of **[6a]**[$TFA]_2$. This process was repeated twice.

Data of [**5**][TFA]:

^{1}H NMR (CD_3CN, 500 MHz): δ (ppm) = 7.84 (*d*, J = 7.7 Hz, 1 H, H_6); 7.65 (*td*, J_1 = 7.4 Hz, J_2 = 1.1 Hz, 1 H, H_4); 7.60 (*d*, J = 7.5 Hz, 1 H, H_7); 7.53 (*t*, J = 7.2 Hz, 1 H, H_5); 6.30 (*t*, J = 5.3 Hz, 1 H, H_{10}); 6.29 (*t*, J = 5.2 Hz, 1 H, H_{13}); 6.10 (*t*, J = 5.6 Hz, 2 H, H_{12}); 6.02 (*t*, J = 5.5 Hz, 2 H, H_{11}); 5.88 (*d*, J = 5.8 Hz, 2 H, H_{14}); 5.82 (*d*, J = 5.8 Hz, 2 H, H_{15}); 5.08 (*s*, 2 H, H_{16}). **^{13}C NMR** (CD_3CN, 125 MHz): δ (ppm) = 169.9 (1 C, C_1); 141.9 (1 C, C_2); 134.8 (1 C, C_3); 132.9 (1 C, C_4); 129.4 (1 C, C_5); 125.2 (1 C, C_6); 123.7 (1 C, C_7); 116.5 (1 C, C_8); 85.3 (1 C, C_9); 84.7 (1 C, C_{10}); 81.3 (2 C, C_{11}); 81.2 (2 C, C_{12}); 79.6 (1 C, C_{13}); 79.5 (2 C, C_{14}); 75.9 (2 C, C_{15}); 57.5 (1 C, C_{16}). **FT-IR** (neat) ν [cm^{-1}]: 3433, 3370, 3063, 3024, 1713, 1622 (C=N), 1442, 1383, 1199, 1130, 838, 734, 659. **UV/Vis** (CH_2Cl_2):λ_{max} 238 nm 21.1×10^3 $M^{-1}cm^{-1}$, λ_{max} 264 nm 12.1 ×10^3 $M^{-1}cm^{-1}$.

HR-ESI-MS: $C_{20}H_{16}N_2Re$; $[M]^+$; calc.: 471.08655 m/z, found: 471.08707 m/z (1.11 Δ ppm). **UV/Vis** (CH_2Cl_2): λ_{max} 264 nm 1.92 ×10^4 $M^{-1}cm^{-1}$. **Elemental Analysis:** [**5**][PF_6] ($C_{20}H_{16}F_6N_2PRe$) calc.: 39.03% C; 2.62% H; 4.55% N. found: 41.77% C; 3.01% H; 4.28% N.

Data of [**6a**][TFA]$_2$ and [**6b**][TFA]$_2$ (2.75:1 mixture):

FT-IR (neat) ν [cm^{-1}]: 3088, 2919, 2854, 1684, 1641, 1517, 1454, 1382, 1200, 1125, 838, 718, 658. **HR-ESI-MS**: $C_{40}H_{32}N_4Re_2$; $[M]^{2+}$; calc.: 471.08655 m/z, found: 471.08664 m/z (0.19 Δ ppm).

Data of [**6a**][TFA]$_2$:

^{1}H NMR (CD_3CN, 500 MHz): δ (ppm) = 7.73 (br. *d*, J = 5.1 Hz, 2 H, H_{15}); 7.64 – 7.51 (*m*, 2x2 H, H_3 and H_7); 7.31 (*d*, J = 3.5 Hz, 2x2 H, H_5 and H_6); 6.40 (*d*, J = 5.3 Hz, 2 H, H_{18}); 6.30 (*d*, J = 5.6 Hz, 2 H, H_{19}); 6.20 (*d*, J = 5.1 Hz, 2 H, H_{16}); 6.14 (*t*, J = 5.2 Hz, 2 H, H_{17}); 6.01 – 5.93 (*m*, 2x2 H, H_{12} and H_{14}); 5.88 – 5.84 (*m*, 2x2 H, H_{10} and H_{13}); 5.68 (*t*, J = 5.3 Hz, 2 H, H_{11}); 5.01 (*d*, J = 16.3 Hz, 2 H, H_{20a}); 4.74 (*d*, J = 16.5 Hz, 2 H, H_{20b}). **^{13}C NMR** (CD_3CN, 125 MHz): δ (ppm) = 159.0 (C_q, 1 C, C_1); 142.1 (C_q, 1 C, C_2); 133.0 (C_q, 1 C, C_3); 130.1 (1 arom. CH, C_4); 128.9 (1 arom. CH, C_5); 127.5 (1 arom. CH, C_6); 124.6 (1 arom. CH, C_7); 119.6 (C_q, 1 C, C_8); 104.7 (C_q, 1 C, C_9); 78.3 (1 arom. CH, C_{10}); 77.6 (1 arom. CH, C_{11}); 76.6 (1 arom. CH, C_{12}); 76.2 (1 arom. CH, C_{13}); 75.6 (1 arom. CH, C_{14}); 75.2 (1 arom. CH, C_{15}); 75.0 (1 arom. CH, C_{16}); 73.9 (1 arom. CH, C_{17}); 72.2 (1 arom. CH, C_{18}); 69.4 (1 arom. CH, C_{19}); 53.7(1 C, CH_2, C_{20}). **UV/Vis** (CH_2Cl_2): λ_{max} 276 nm 377.3 ×10^3 $M^{-1}cm^{-1}$. **FT-IR** (neat) ν [cm^{-1}]: 3095, 2933, 2857, 1691, 1634, 1515, 1455, 1388, 1202, 1128, 1057, 841, 727. **UV/Vis** (CH_2Cl_2): λ_{max} 250 nm 1.25 ×10^4 $M^{-1}cm^{-1}$; λ_{max} 288 nm 1.64 ×10^4 $M^{-1}cm^{-1}$. **Elemental Analysis:** [**6a**][TFA]$_2$(H_2O)$_3$ ($C_{44}H_{38}F_6N_4O_7Re_2$) calc.: 43.28% C; 3.14% H; 4.59% N. found: 42.55% C; 2.51% H; 4.62% N.

Data of [**6b**][TFA]$_2$:

^{1}H NMR (CD_3CN, 500 MHz): δ (ppm) = 7.73 (br. *d*, J = 5.1 Hz, 2 H, H_{15}); 7.64 – 7.51 (*m*, 2x2 H, H_{15} and H_7); 7.31 (*d*, J = 3.5 Hz, 2x2 H, H_5 and H_6); 6.40 (*d*, J = 5.3 Hz, 2 H, H_{18}); 6.30 (*d*, J = 5.6 Hz, 2 H, H_{19}); 6.20 (*d*, J = 5.1 Hz, 2 H, H_{16}); 6.14 (*t*, J = 5.2 Hz, 2 H, H_{17}); 6.01 – 5.93 (*m*, 2x2 H, H_{12} and H_{14}); 5.88 – 5.84 (*m*, 2x2 H, H_{10} and H_{13}); 5.68 (*t*, J = 5.3 Hz, 2 H, H_{11}); 5.01 (*d*, J = 16.3 Hz, 2 H, H_{20a}); 4.74 (*d*, J = 16.5 Hz, 2 H, H_{20b}).

^{13}C NMR (CD_3CN, 125 MHz): δ (ppm) = 159.0 (C_q, 1 C, C_1); 142.1 (C_q, 1 C, C_2); 133.0 (C_q, 1 C, C_3); 130.1 (1 arom. CH, C_4); 128.9 (1 arom. CH, C_5); 127.5 (1 arom. CH, C_6); 124.6 (1 arom. CH, C_7); 119.6 (C_q, 1 C, C_8); 104.7 (C_q, 1 C, C_9); 78.3 (1 arom. CH, C_{10}); 77.6 (1 arom. CH, C_{11}); 76.6 (1 arom. CH, C_{12}); 76.2 (1 arom. CH, C_{13}); 75.6 (1 arom. CH, C_{14}); 75.2 (1 arom. CH, C_{15}); 75.0 (1 arom. CH, C_{16}); 73.9 (1 arom. CH, C_{17}); 72.2 (1 arom. CH, C_{18}); 69.4 (1 arom. CH, C_{19}); 53.7(1C, CH_2, C_{20}).

Synthesis of [**7**]$^+$:

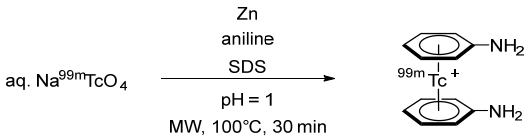

[**7**]$^+$

A MW vial was charged with Zn powder (10.9 mg, 167 µmol), SDS (4.8 mg, 17 µmol), aniline (50 µL), and aq. HCl (3 N, 50 µL). Aq. $Na^{99m}TcO_4$ (generator eluate, 1 mL) was flushed with N_2 for 1 min. The $Na^{99m}TcO_4$ solution was added to the microwave vial and the almost clear solution was heated to 100°C

for 30 min. The reaction solution was filtered into a vial where 36% of the initial activity was recovered. The pH of the transferred solution was 6 which was neutralized with aq. NaOH (1 N, 30 µL). (Note: neutralization is helpful in this case to improve chromatographic performance on the analytical HPLC) An aliquot of the reaction mixture was injected onto a radio HPLC to confirm presence of the target material (R_t = 9.98 min; hold 5% B for 3 min, 5% to 25% B in 0.1 min, hold 25% B for 5.9 min, 25% to 34% B in 0.1 min, 34% to 100% B in 11.9 min, hold 100% CH_3CN for 5 min, 100% to 5% CH_3CN in 0.1 min, hold 5% CH_3CN for 4.9 min/250 nm). The crude reaction mixture was concentrated to around 0.4 mL under N_2 stream to give a milky suspension. The suspension was diluted with CH_3CN (0.2 mL) and H_2O (0.1 mL) which resulted in a clear solution. To isolate [**7**]$^+$, 70 µL of the clear solution was injected onto the radio HPLC and the peak containing the target material was collected (R_t = 18.13 min; hold 5% B for 5 min, 5% to 35%B in 40 min, hold 35% B for 5 min, 35% to 100% B in 10 min, 100% to 10% B in 2 min, hold 100% B for 3 min).

Synthesis of [^{99m}Tc][**5**]$^+$:

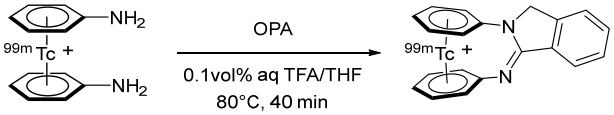

[**7**]$^+$ [^{99m}Tc][**5**]$^+$

O-Phthalaldehyde (50 µL) from a stock solution (stock: 5.6 mg *o*-phthalaldehyde in 200 µL THF) was added into an aq. solution of **[7]**$^+$ (3 mL). The clear solution was stirred at 80 °C for 40 min. The solution was concentrated under N_2 stream, then 100 µL of the solution was injected into HPLC using gradient (R_t = 27.30 min; hold 5% CH_3CN for 5 min, 5% to 60% CH_3CN in 30 min, hold 60% CH_3CN for 5 min, 60% to 100% CH_3CN in 2 min, hold 100% CH_3CN for 3 min/250 nm). Peaks containing the target materials were collected. The identity of **[**[^{99m}Tc][**5**]$^+$ was confirmed through co-injection of an aliquot of the collected material with [**5**][TFA] onto the radio HPLC (R_t = 15.85 min; hold 5% B for 3 min, 5% to 25% B in 0.1 min, hold 25% B for 5.9 min, 25% to 34% B in 0.1 min, 34% to 100% B in 11.9 min, hold 100% B for 5 min, 100% to 5% B in 0.1 min, hold 5% B for 4.9 min/270 nm).

Synthesis of [**8**][TFA]:

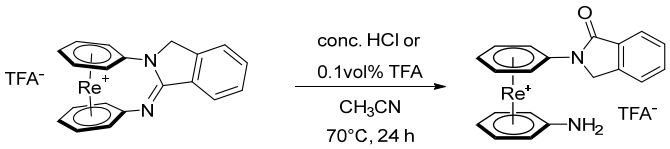

[**5**][TFA] [**8**][TFA] (77%)

A Schlenk Flask equipped with a stir bar and a septum was charged with CH_3CN (1 mL) and [**5**][TFA] (1.0 mg, 1.8 mmol, 1.0 eq). Conc. HCl (32%, 10 mL) was added, and the reaction mixture was heated to 70°C for 24 h. The crude reaction mixture was purified by preparative HPLC (21.7 min; hold 5% CH_3CN for 3 min, 5% to 50% CH_3CN in 30 min, 50% to 100% CH_3CN in 2 min, hold 100% CH_3CN for 3 min/270 nm). Fractions containing the target material were collected and lyophilized. The title compound [**8**][TFA] (0.8 mg, 1.4 µmol, 77%) was obtained as yellow powder. The same result was obtained when [**5**][TFA] was heated in 0.1 vol% aq. TFA to 110°C for 3 h in the micro wave. No hydrolysis was observed when [**5**][TFA] was stirred in 0.1 vol% aq. TFA for 24 h at 25°C. . The counter

ion was exchanged to PF_6^- by addition of sat. aq. NH_4PF_6 to a solution of [**5**][TFA]. [**5**][PF_6] precipitated and was filtered off.

Data of [**8**][TFA]:

^{1}H NMR (CD_3CN, 400 MHz): δ (ppm) 7.82 (*d*, J = 7.8 Hz, 1 arom. CH); 7.72 (*td*, J = 7.8, 1.1 Hz, 1 arom. CH); 7.63 (*dt*, J = 7.6, 0.7 Hz, 1 arom. CH); 7.57 (*d*, J = 7.7 Hz, 1 arom. CH); 6.72 (*d*, J = 6.0 Hz, 2 arom. CH); 5.95 (*d*, J = 5.9 Hz, 2 arom. CH); 5.87 (*t*, J = 5.6 Hz, 2 arom. CH); 5.80 (*t*, J = 5.7 Hz, 2 arom. CH); 5.64 (*t*, J = 5.2 Hz, 1 arom. CH); 5.57 (*t*, J = 5.2 Hz, 1 arom. CH); 4.71 (*s*, 2 H, CH). **HR-ESI-MS**: $C_{20}H_{18}N_2ORe$; $[M]^+$; calc.: 489.09712 m/z, found: 489.09751m/z (0.80 Δ ppm). **UV/Vis** (CH_2Cl_2): λ_{max} 286 nm 4.21 ×10^4 $M^{-1}cm^{-1}$. **Elemental Analysis:** [**8**][PF_6] ($C_{20}H_{18}F_6N_2OPRe$) calc.: 37.92% C; 2.86% H; 4.42% N. found: 38.99% C; 2.78% H; 4.59% N.

2 Spectroscopic Data

2.1 NMR Spectra

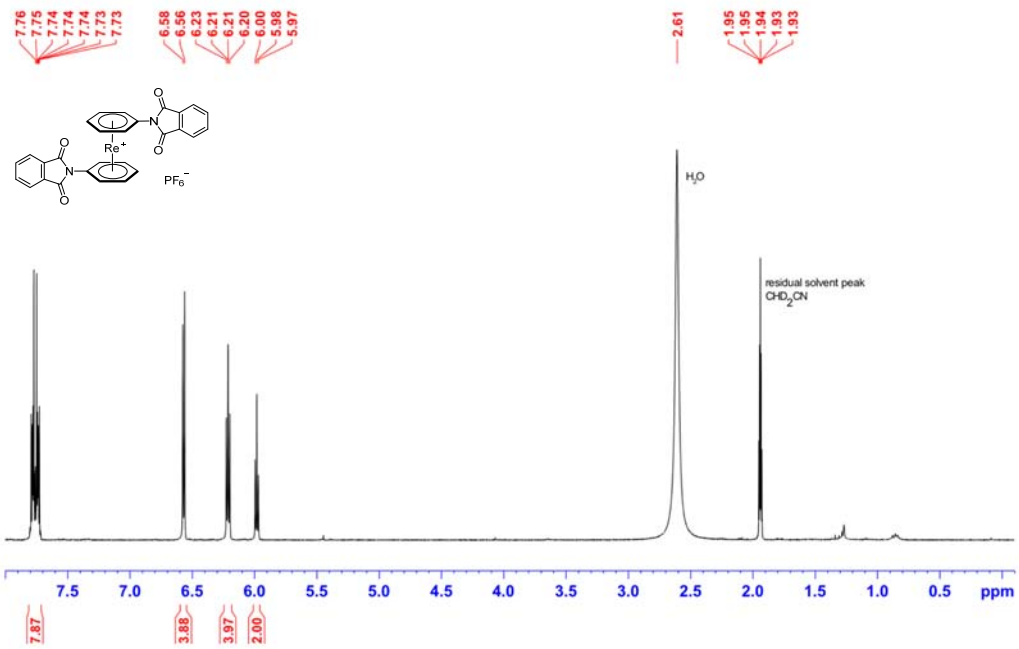

Figure S1: ^{1}H NMR of [**3**][PF_6] in CD_3CN (400 MHz, 298K).

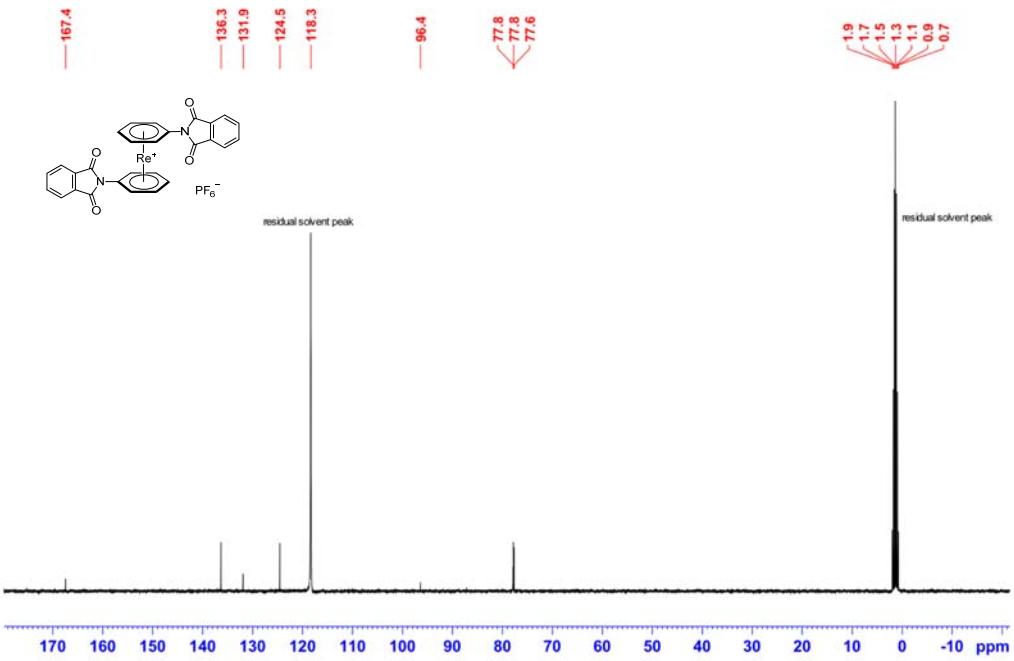

Figure S2: ^{13}C NMR of [**3**][PF_6] in CD_3CN (100 MHz, 298K).

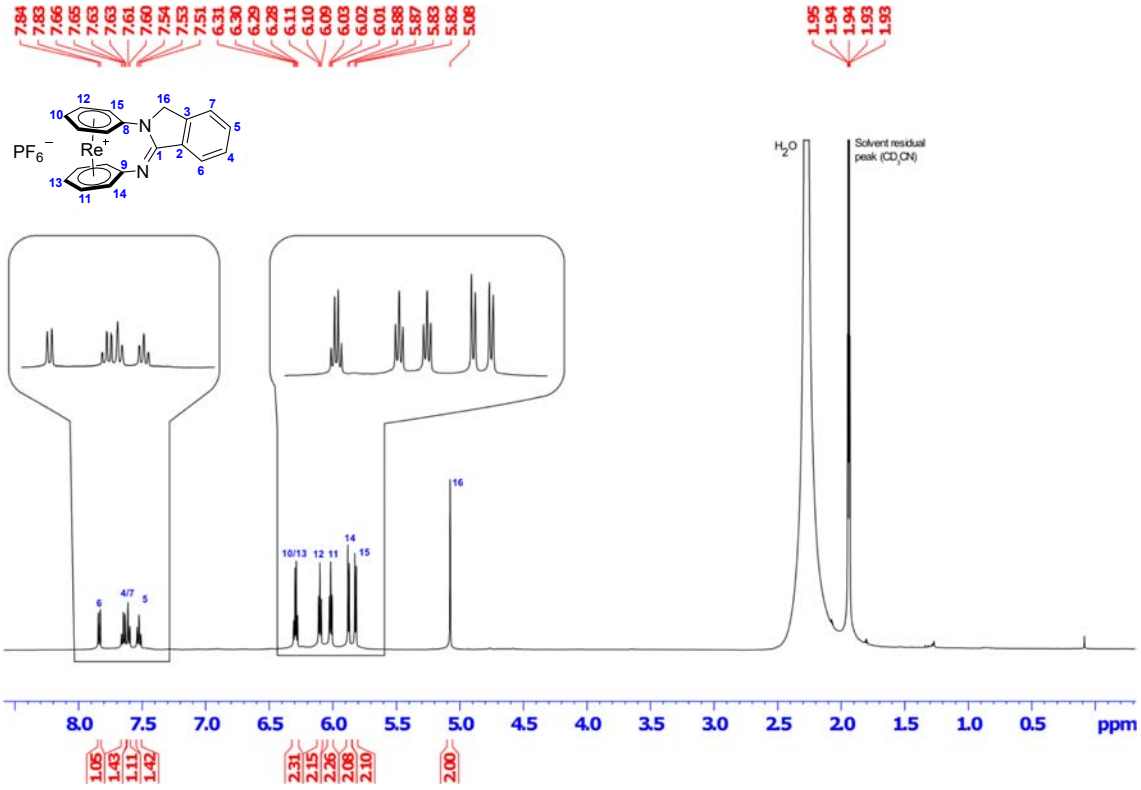

Figure S3: ^{1}H NMR of [**5**][PF_6] in CD_3CN (500 MHz, 298K).

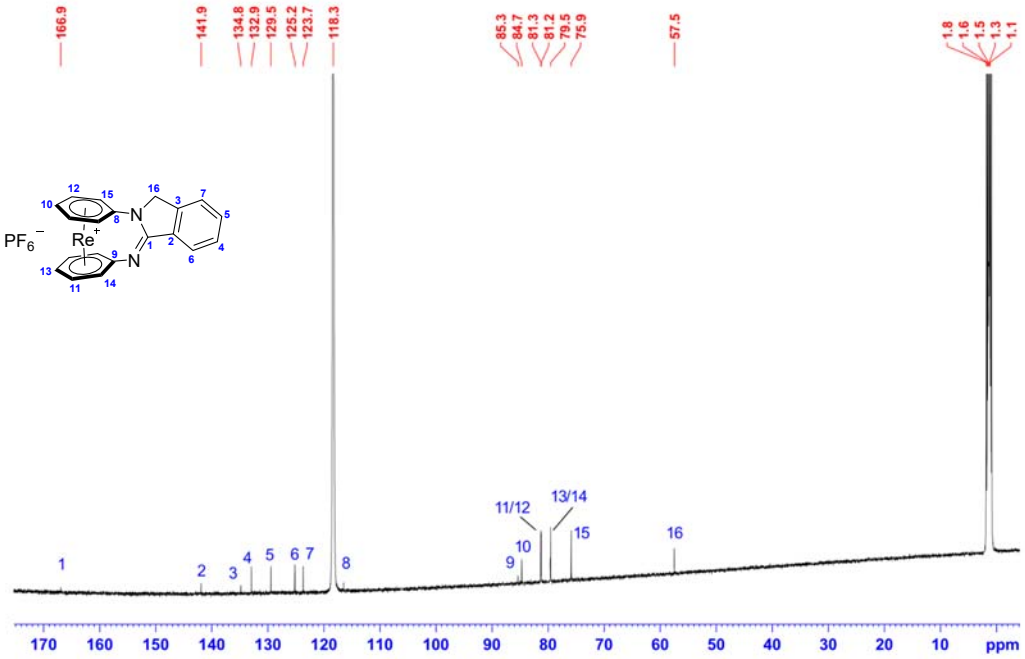

Figure S4: ^{13}C NMR of [**5**][PF_6] in CD_3CN (100 MHz, 298K).

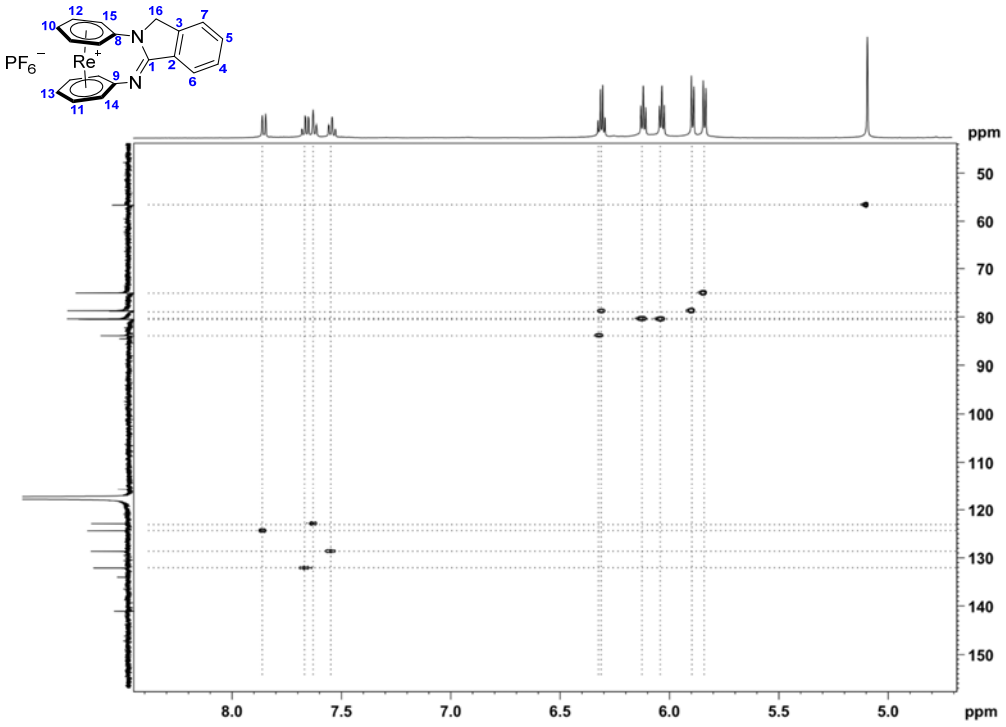

Figure S5: HSQC correlation spectrum of [**5**][PF_6] in CD_3CN (298K).

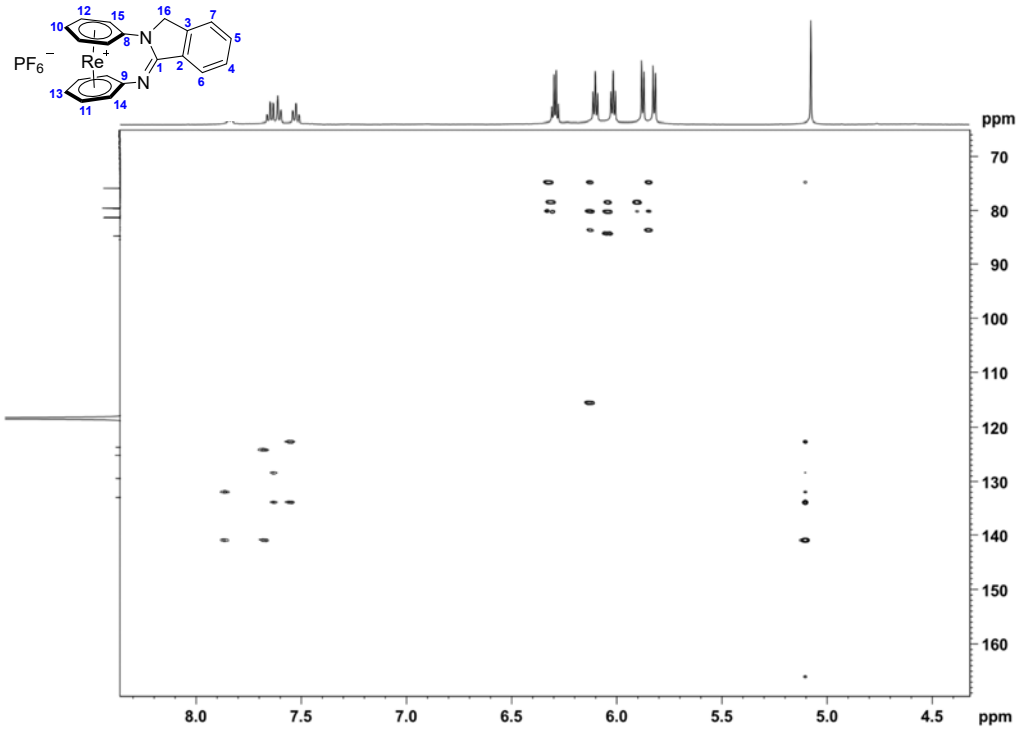

Figure S6: HSQC correlation spectrum of [**5**][PF_6] in CD_3CN (298K)

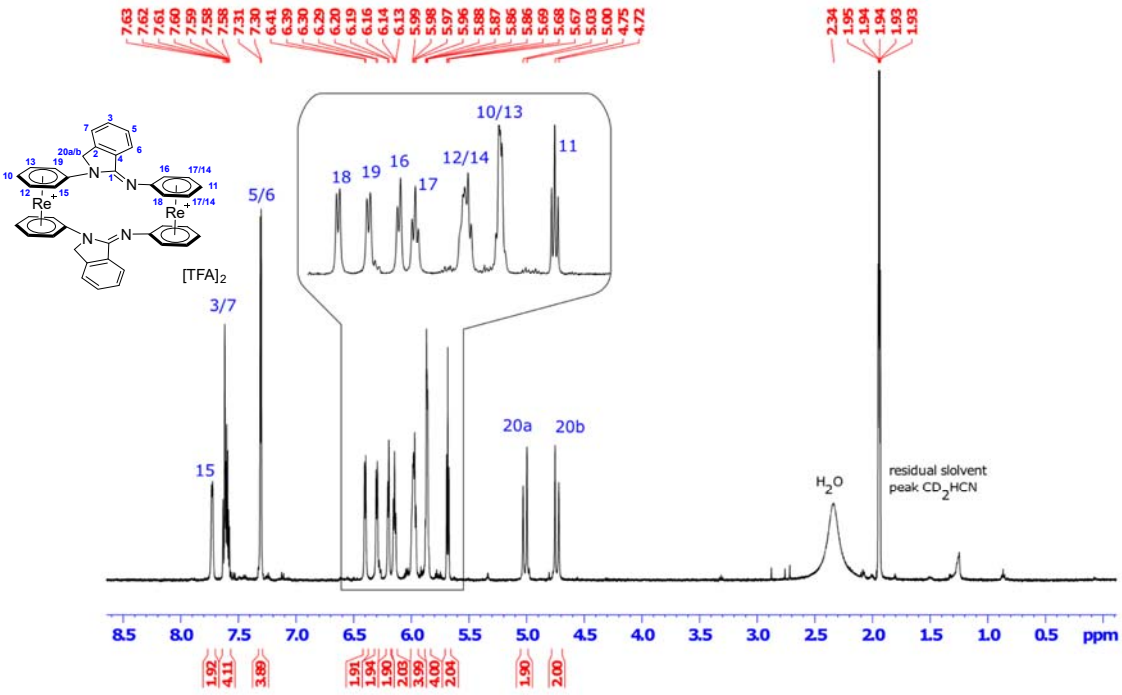

Figure S7: ^1H NMR of [**6a**][TFA]$_2$ in CD_3CN (500 MHz, 270K).

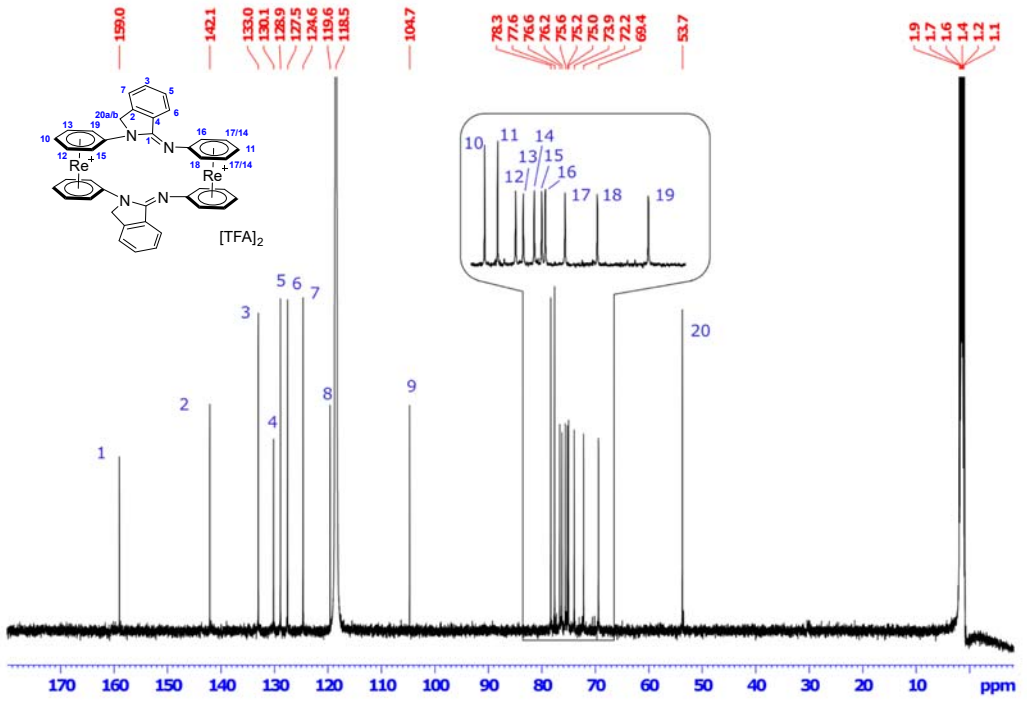

Figure S8: ^{13}C NMR of [**6a**][TFA]$_2$ in CD_3CN (125 MHz, 270K).

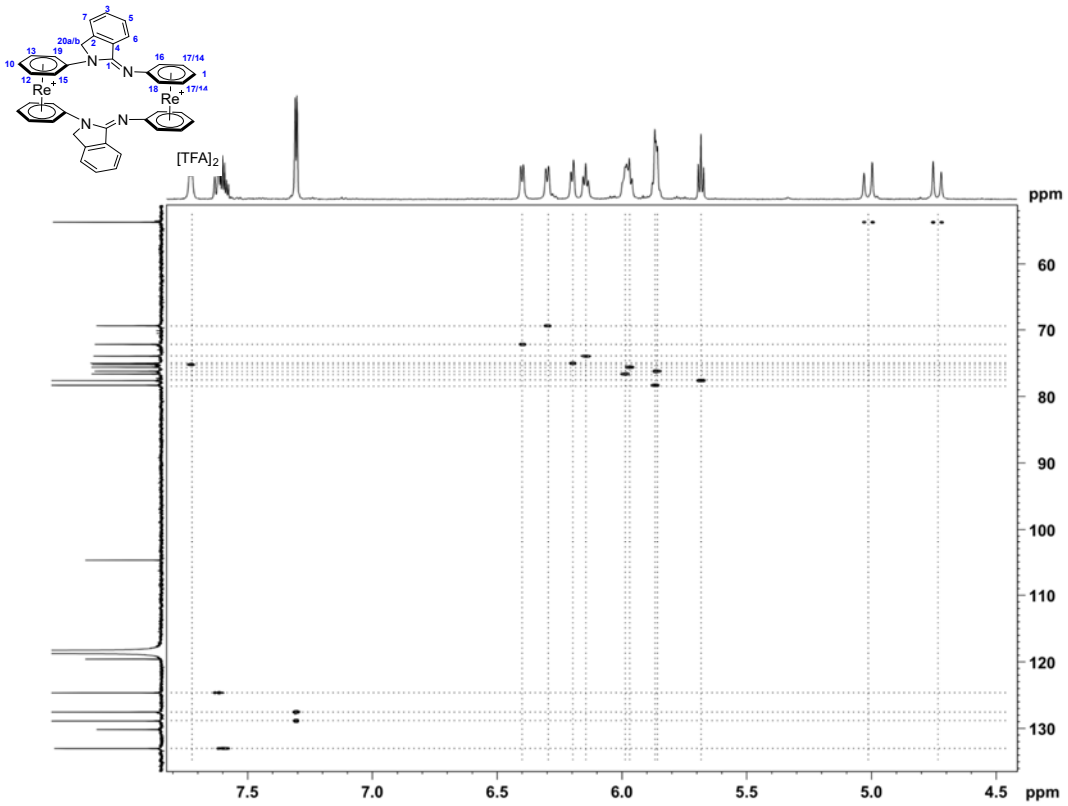

Figure S9: HSQC correlation spectrum of [**6a**][TFA]$_2$ in CD_3CN (270K).

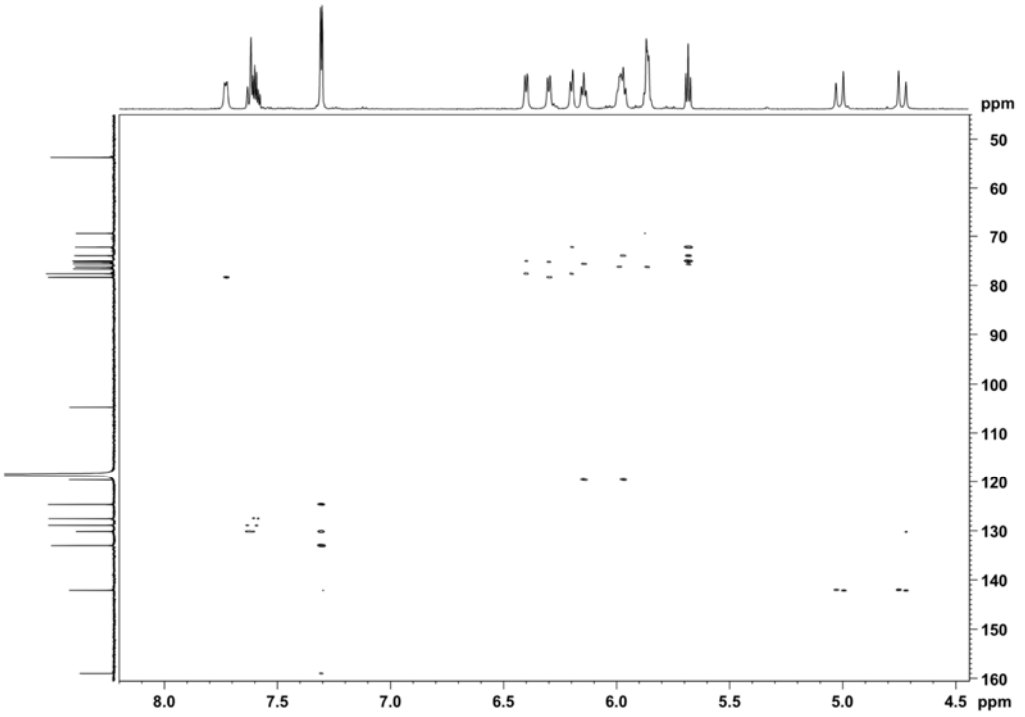

Figure S10: HMBC correlation spectrum of [**6a**][TFA]$_2$ in CD_3CN (270K).

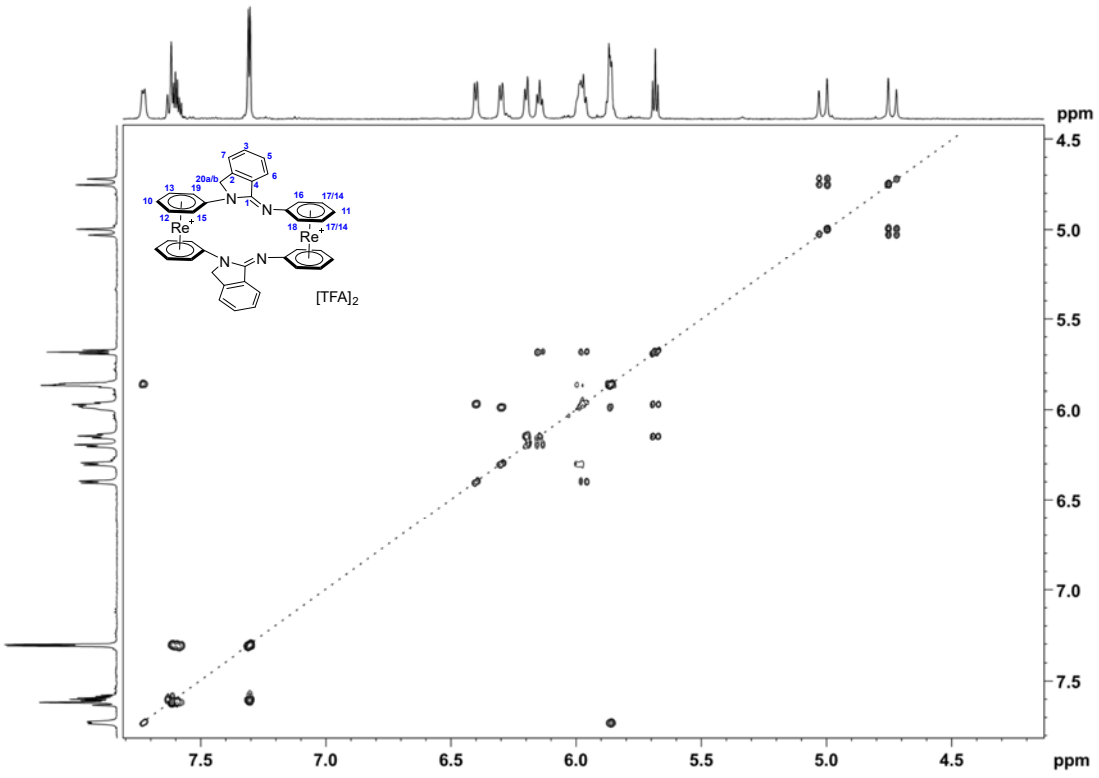

Figure S11: COSY correlation spectrum of [**6a**][TFA]$_2$ in CD_3CN (270K).

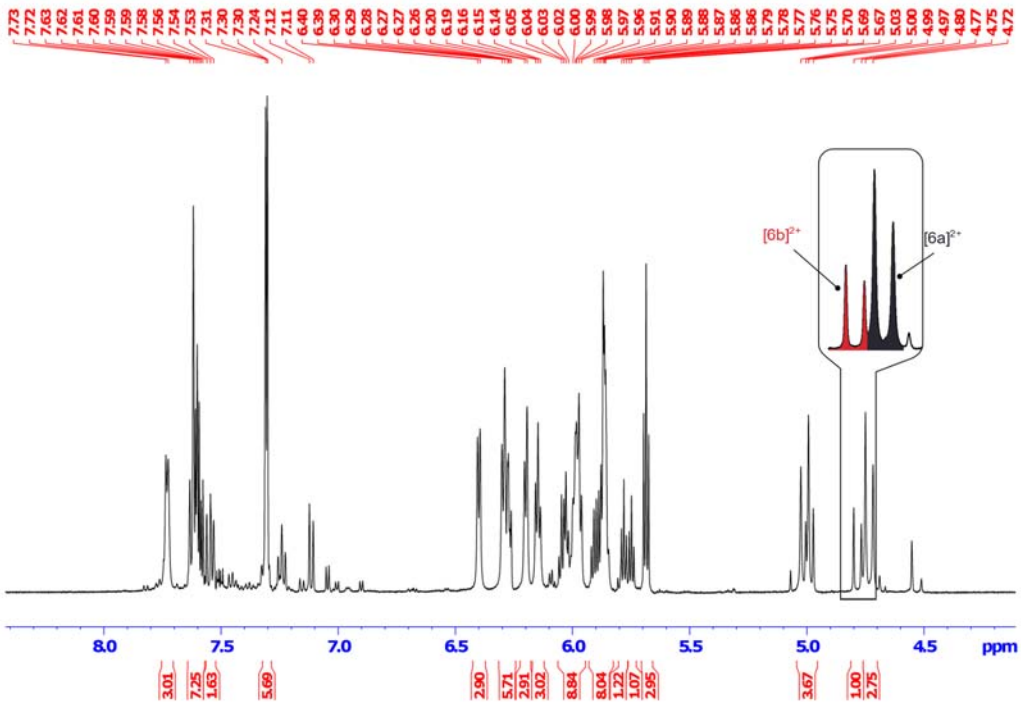

Figure S12: ^{1}H NMR of a 2.75:1 molar ratio mixture of [**6a**][TFA]$_2$ and [**6b**][TFA]$_2$ in CD_3CN (500 MHz, 270K).

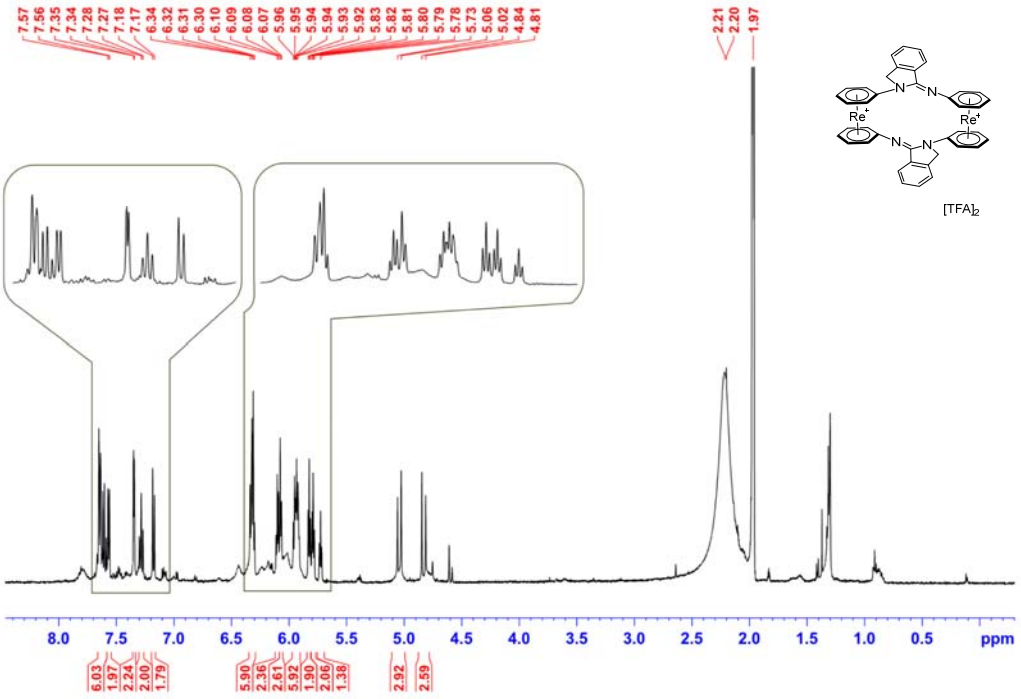

Figure S13: ^{1}H NMR of [**6b**][TFA]$_2$ in CD_3CN (500 MHz, 298K), contaminated with [**6a**][TFA]$_2$.

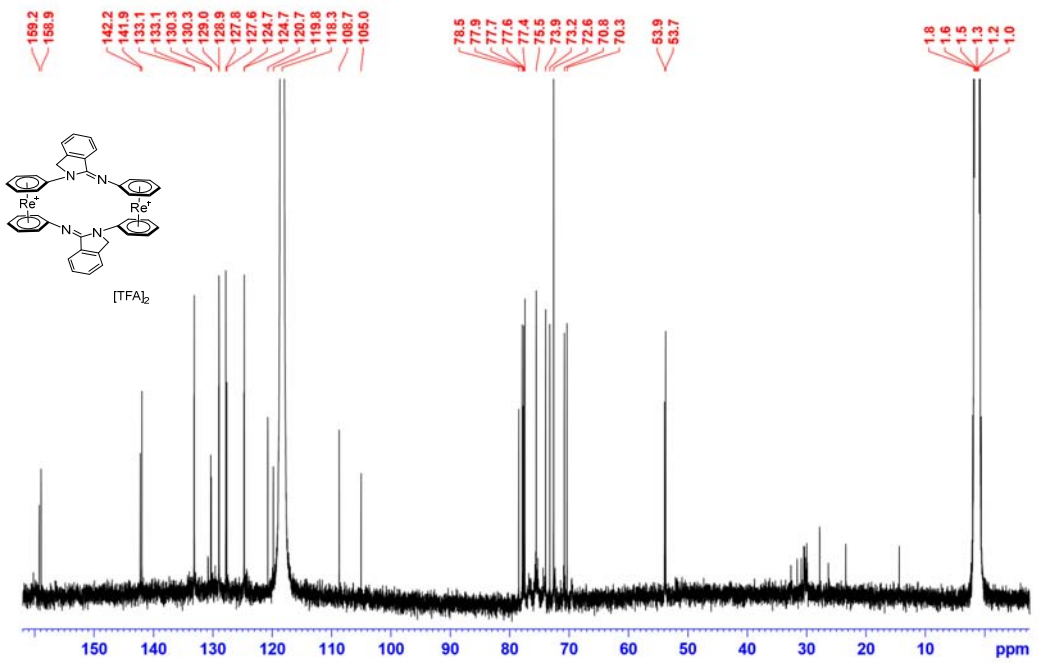

Figure S14: ^{1}H NMR of [**6b**][TFA]$_2$ in CD_3CN (125 MHz, 298 K), contaminated with [**6a**][TFA]$_2$.

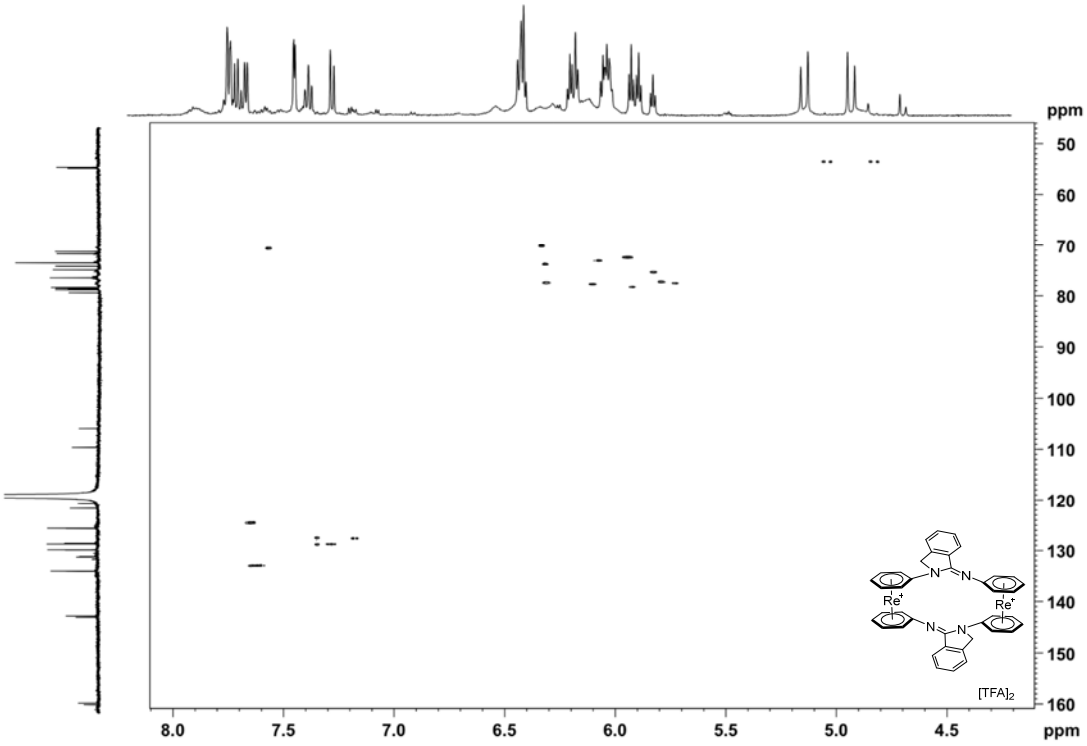

Figure S15: HSQC correlation spectrum of [**6b**][TFA]$_2$ in CD_3CN (298K), contaminated with [**6a**][TFA]$_2$.

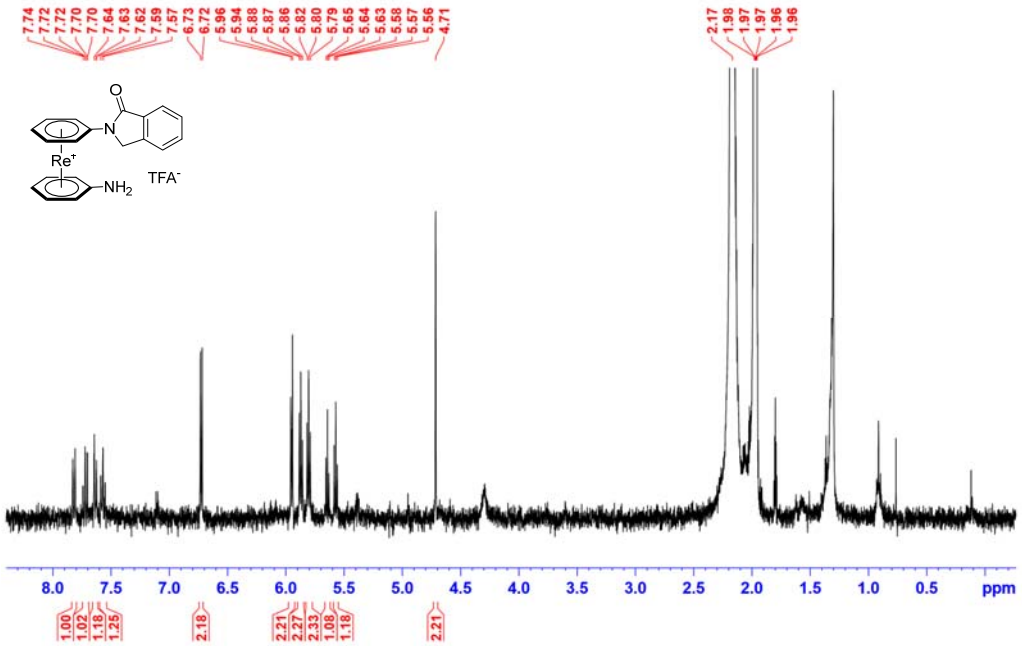

Figure S16: ^{1}H NMR of [**8**][TFA] in CD_3CN (400 MHz, 398K).

2.2 IR Spectra

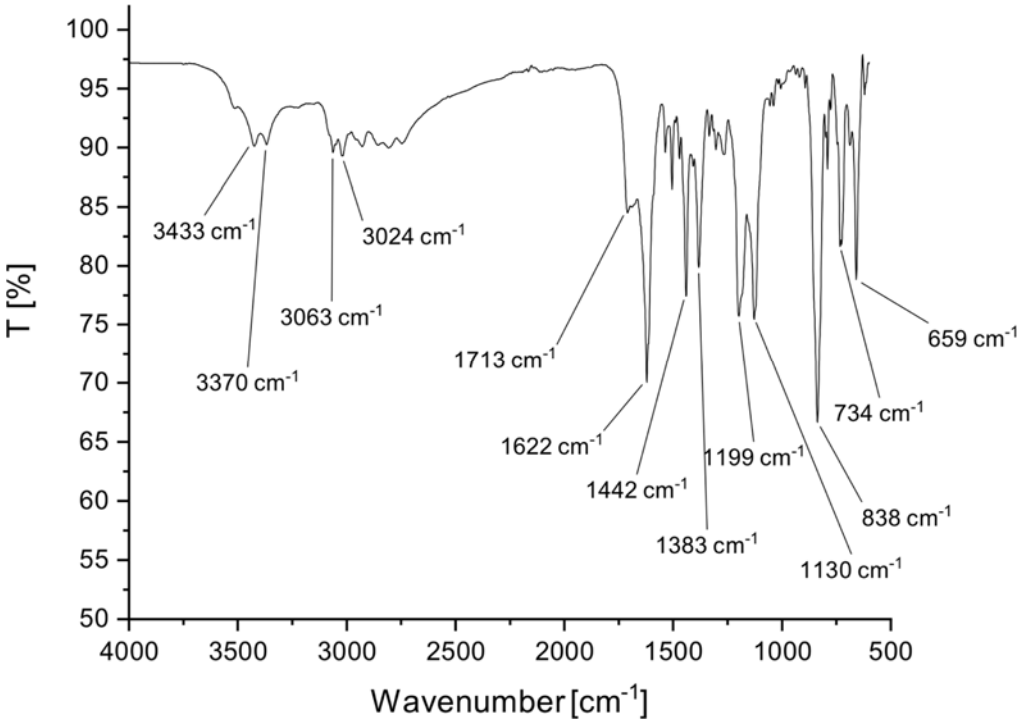

Figure S17: FT-IR spectrum of [**5**][PF_6] (neat).

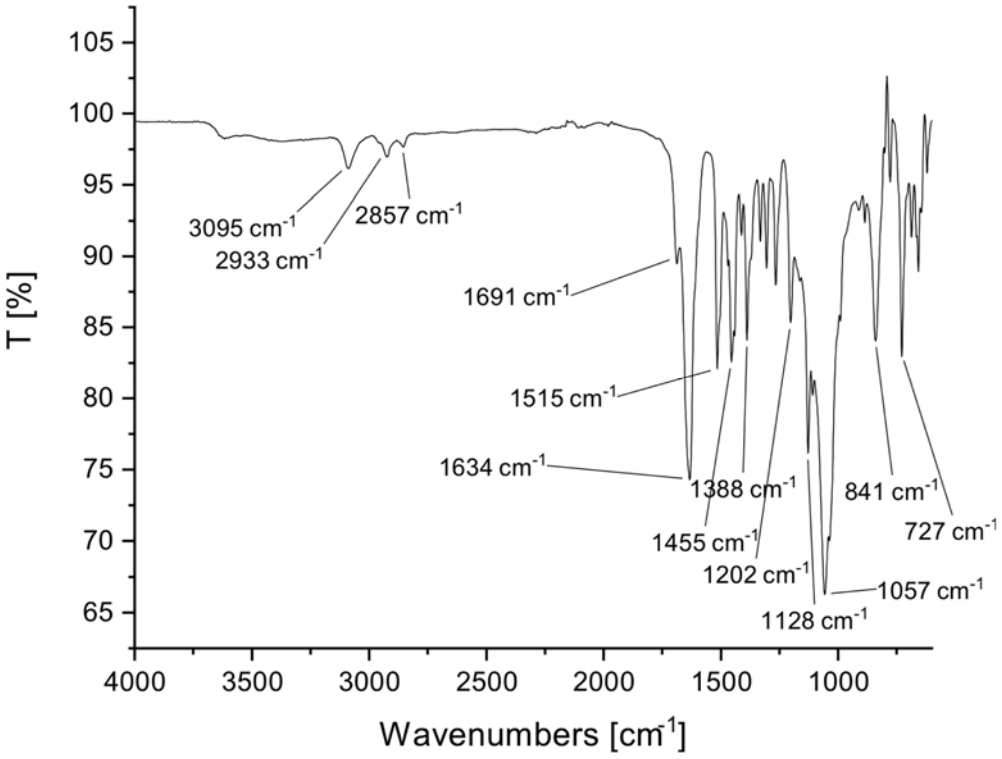

Figure S18: FT-IR spectrum of [**6a**][TFA]$_2$ (neat).

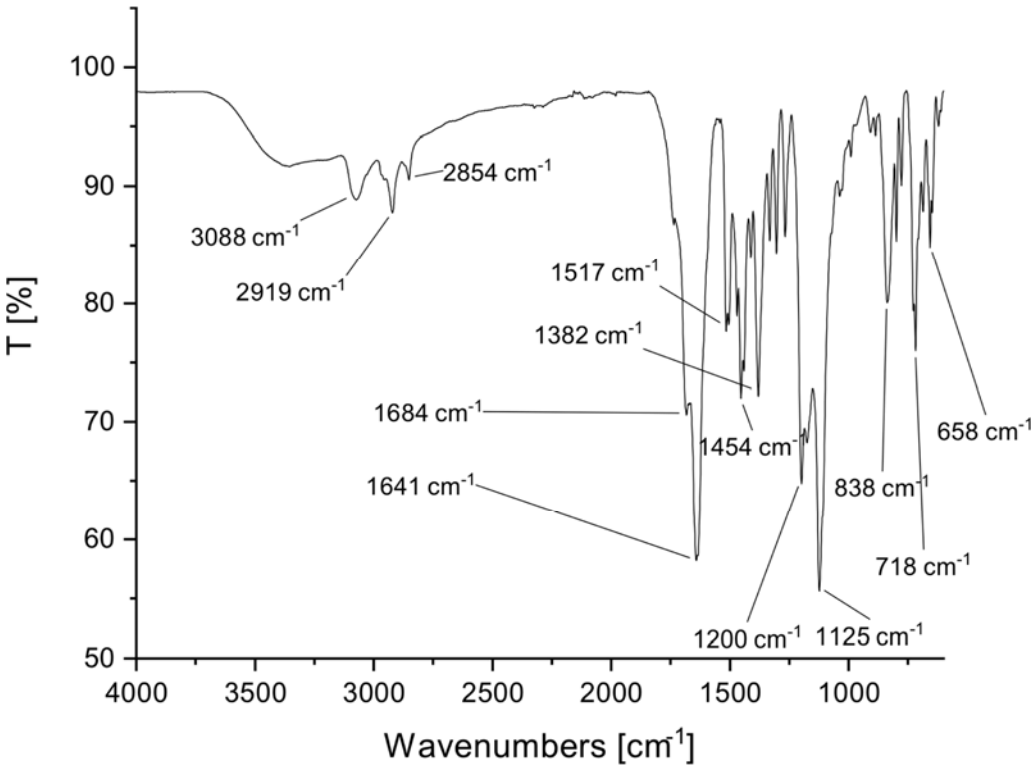

Figure S19: FT-IR spectrum of a 2.75:1 molar ratio mixture of [**6a**][TFA]$_2$ and [**6b**][TFA]$_2$ (neat).

2.3 HR-ESI-MS

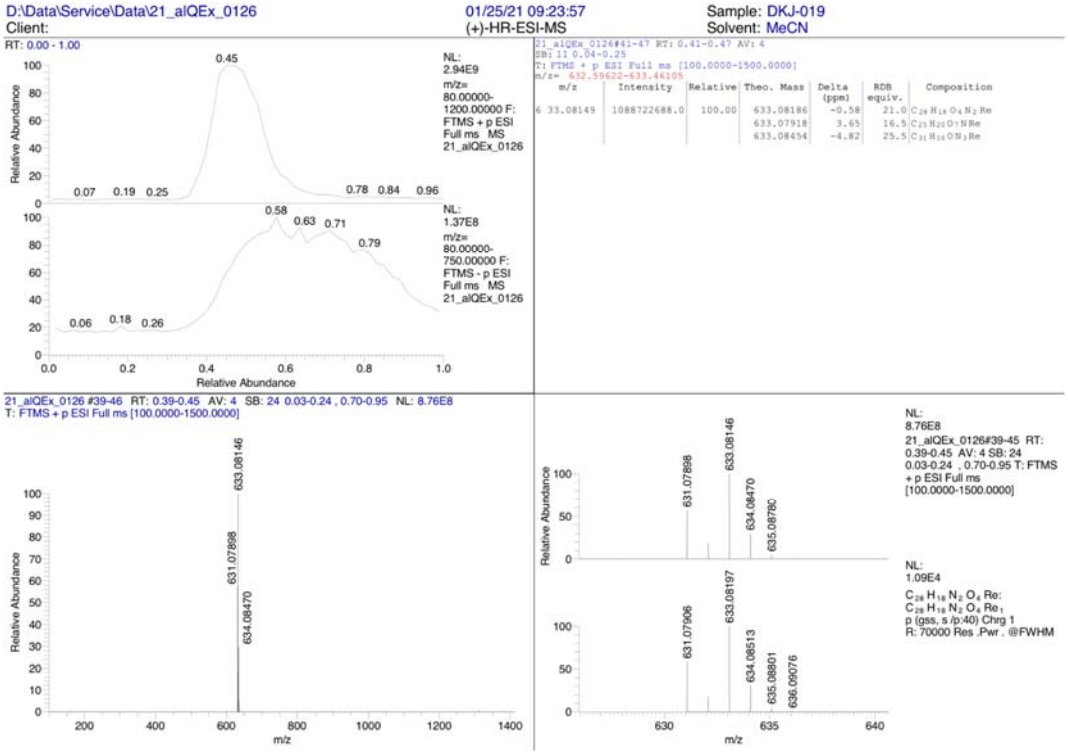

Figure S20: (+)-HR-ESI-MS data of [**3**]$^+$.

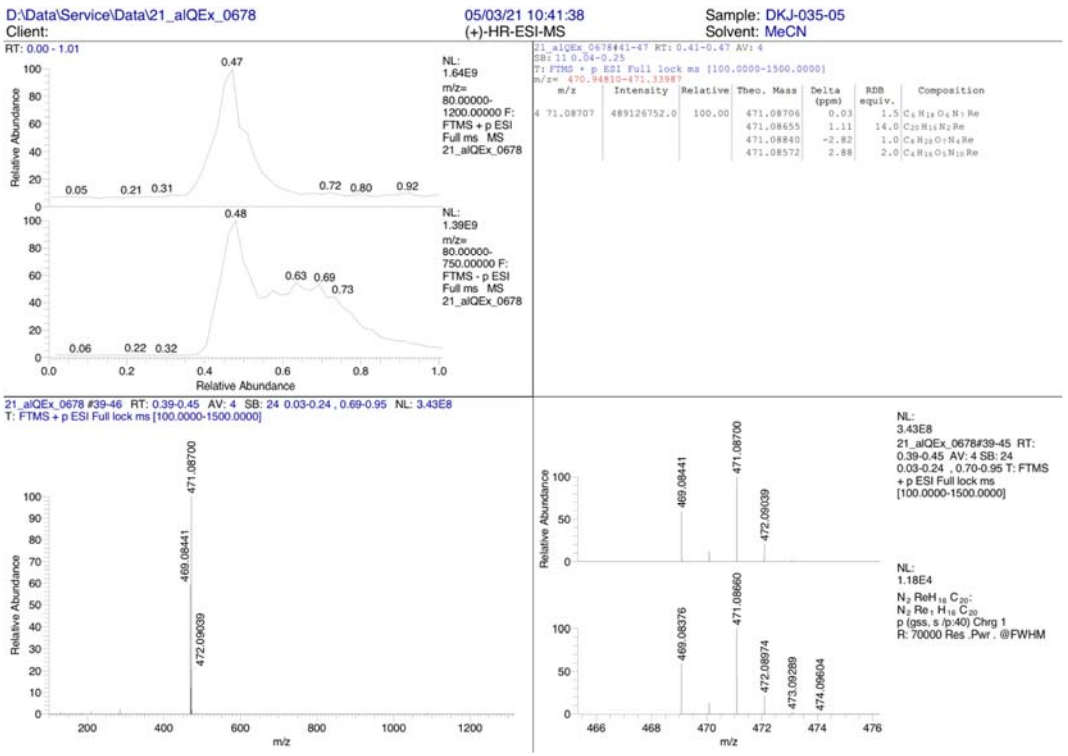

Figure S21: (+)-HR-ESI-MS data of [**5**]$^+$.

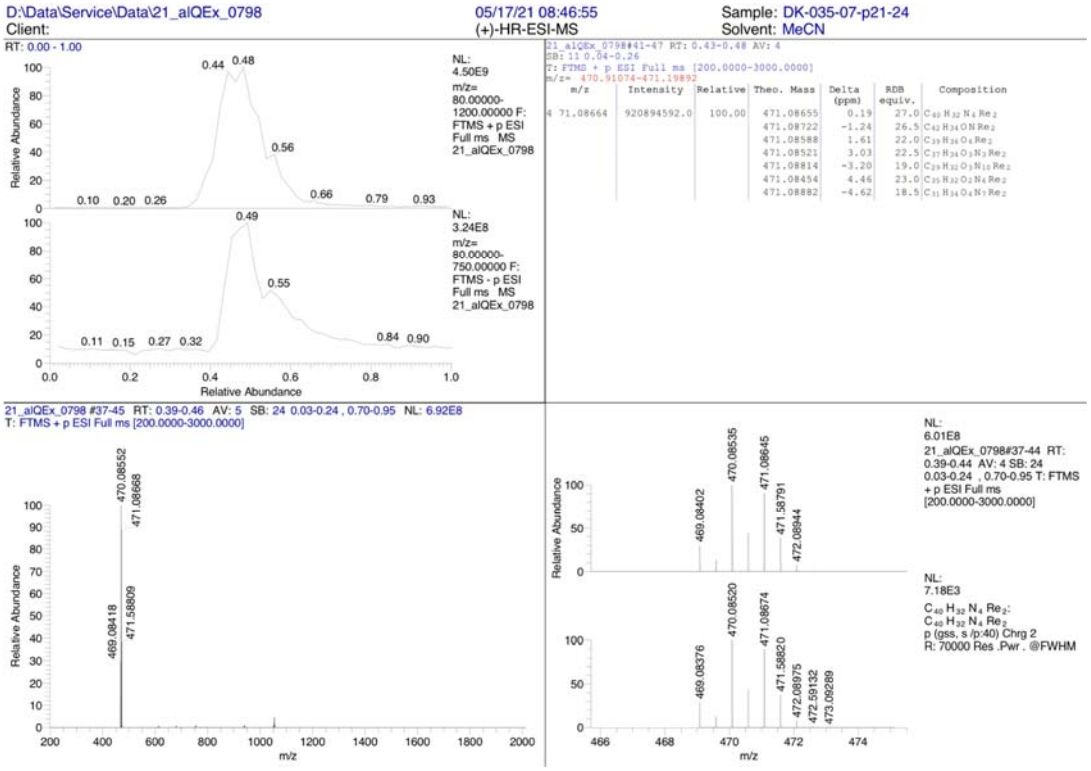

Figure S22: (+)- HR-ESI-MS data of [**6a**]$^{2+}$ and [**6b**]$^{2+}$ (data recorded of a 2.75:1 molar mixture).

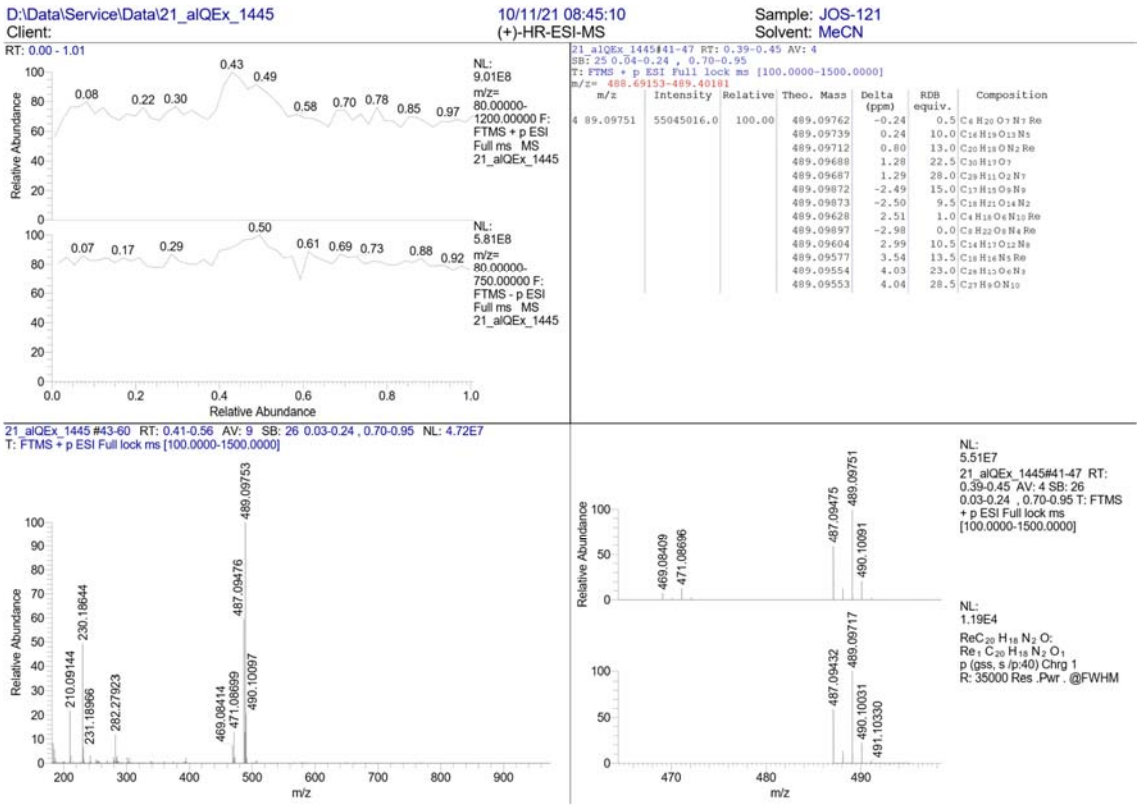

Figure S 23: (+)- HR-ESI-MS data of [**8**]$^{+}$.

2.4 Crystallographic Data

Data of [**3**][PF_6]

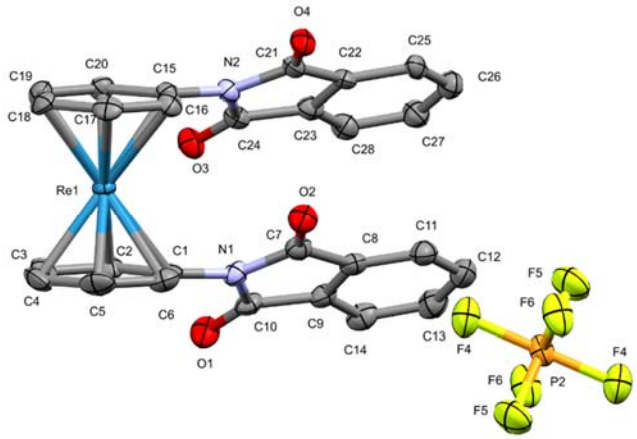

Figure S24: ORTEP representation of [**3**][PF_6]. Ellipsoids represent 50% probability. Hydrogen atoms are omitted for clarity

Special features: The crystal structure was refined as a two-component non-merohedral twin [scale: 0.1760(5) / 0.8240(5)]. The minor component was rotated by 179.99° around [0.0 1.0 0.0] in the reciprocal space or around [0.17 0.97 0.20] in the direct space.

Table S1: Tabulated values of selected bond lengths and angles of the crystallographic data of **[3]**[PF_6].

Selected bond lengths [Å]		Selected angles [°]	
Centroid-Re-Centroid	1.732(3)/1.736(3)	Centroid-Re-Centroid	179.02
C15-N2	1.418(7)	C7-N1-C10	126.4(4)
C21-N2	1.432(6)	N1-C10-C9	106.4(4)
C24-N2	1.427(7)		
C10-O1	1.207(7)		

Table S2: Crystallographic data and structure refinement for [3][PF_6]	
Identification code	**[3][PF_6]**
Empirical formula	$C_{28}H_{18}F_6N_2O_4PRe$
Formula weight	777.61
Temperature/K	160(1)
Crystal system	triclinic
Space group	P-1
a/Å	7.1963(3)
b/Å	12.2113(5)
c/Å	14.9263(6)
α/°	102.971(4)
β/°	102.419(4)
γ/°	92.903(4)
Volume/$Å^3$	1241.53(9)
Z	2
$\rho_{calc}g/cm^3$	2.080
μ/mm^{-1}	10.980
F(000)	752.0
Crystal size/mm^3	0.08 × 0.04 × 0.02
Radiation	Cu Kα (λ = 1.54184)
2Θ range for data collection/°	6.248 to 154.638
Index ranges	$-9 \le h \le 9$, $-13 \le k \le 15$, $-18 \le l \le 18$
Reflections collected	9155

Independent reflections	9155 [R_{int} = ?, R_{sigma} = 0.0323]
Data/restraints/parameters	9155/0/383
Goodness-of-fit on F^2	1.049
Final R indexes [I>=2σ (I)]	R_1 = 0.0332, wR_2 = 0.0881
Final R indexes [all data]	R_1 = 0.0417, wR_2 = 0.0917
Largest diff. peak/hole / e $Å^{-3}$	1.09/-1.50

Data of [**5**][PF_6]·(CH_3CN)

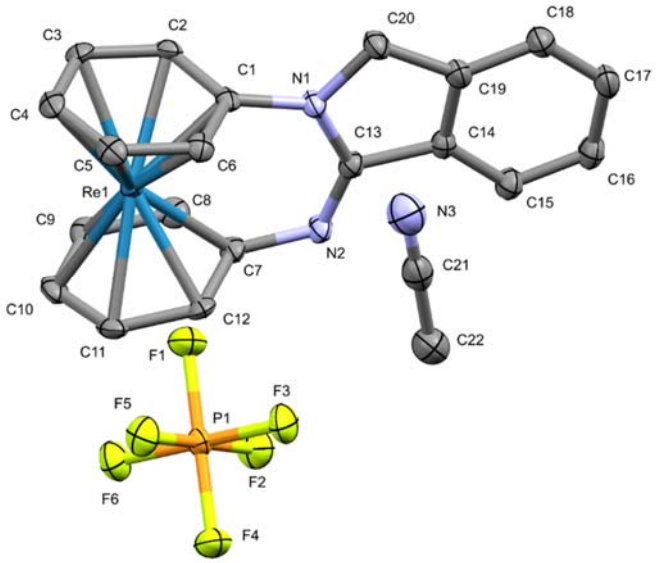

Figure S25: ORTEP representation of [**5**][PF_6](CH_3CN). Ellipsoids represent 50% probability. Hydrogen atoms are omitted for clarity

Table S3: Tabulated values of selected bond lengths and angles of the crystallographic data of **[5]**[PF_6](CH_3CN).

Selected bond lengths [Å]		Selected angles [°]	
Centroid-Re-Centroid	1.7324(11)/1.7159(11)	Centroid-Re-Centroid	145.2(16)
C1-N1	1.419(3)	C1-N1-C13	128.2(2)
C7-N2	1.404(3)	C13-N1-C20	112.8(2)
C13-N1	1.384(3)	C14-C13-N1	118.6(2)
C13-N2	1.292(3)	C7-N2-C13	123.0(2)
C20-N1	1.473(3)		

Table S4: Crystallographic data and structure refinement for [5][PF_6] CH_3CN	
Identification code	**[5][PF_6]**
Empirical formula	$C_{22}H_{19}F_6N_3PRe$
Formula weight	656.57
Temperature/K	160(1)
Crystal system	monoclinic
Space group	$P2_1/c$
a/Å	7.61700(10)
b/Å	31.5018(3)
c/Å	8.58250(10)
α/°	90
β/°	97.1320(10)
γ/°	90
Volume/$Å^3$	2043.43(4)
Z	4
$\rho_{calc}g/cm^3$	2.134
μ/mm^{-1}	13.032
F(000)	1264.0
Crystal size/mm^3	0.3 × 0.14 × 0.03
Radiation	Cu Kα (λ = 1.54184)
2Θ range for data collection/°	5.61 to 149.002
Index ranges	$-9 \le h \le 9$, $-39 \le k \le 39$, $-10 \le l \le 10$
Reflections collected	22813
Independent reflections	4195 [R_{int} = 0.0221, R_{sigma} = 0.0114]
Data/restraints/parameters	4195/0/299
Goodness-of-fit on F^2	1.183
Final R indexes [I>=2σ (I)]	R_1 = 0.0185, wR_2 = 0.0454
Final R indexes [all data]	R_1 = 0.0186, wR_2 = 0.0455
Largest diff. peak/hole / e $Å^{-3}$	0.75/-0.67

Data of [**6a**][TFA]$_2$ H_2O

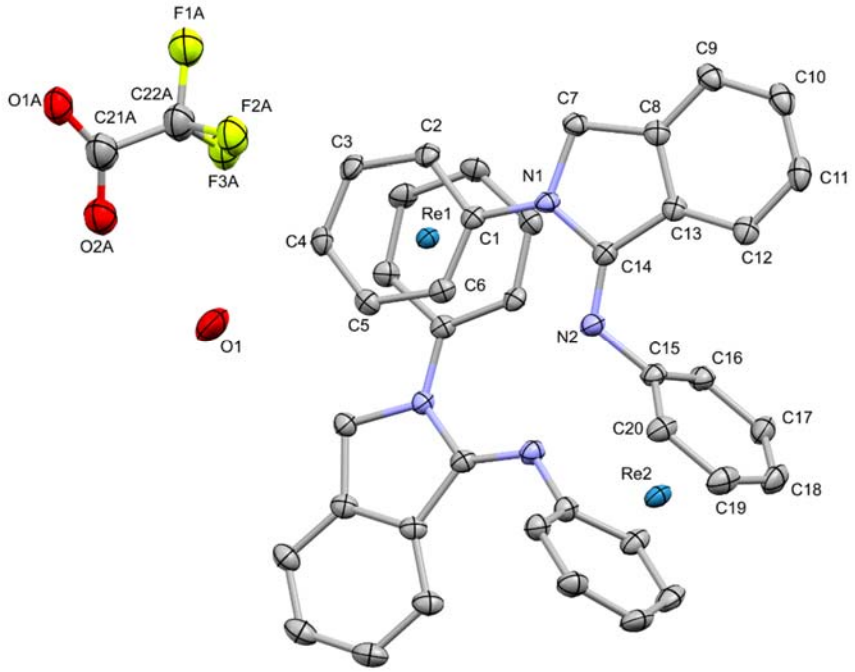

Figure S26: ORTEP representation of [**6a**][TFA]$_2$(H_2O), Ellipsoids represent 30% probability. One TFA molecule and hydrogen atoms are omitted for clarity.

Special features: The two metal centers are located on a two-fold axis.

Table S5: Tabulated values of selected bond lengths and angles of the crystallographic data of **[6a]**[TFA]$_2$ H_2O.

Selected bond lengths [Å]		Selected angles [°]	
Centroid-Re-Centroid	1.739(2)/1.743(3)	Centroid-Re-Centroid	179.94(17)/179.16(15)
C1-N1	1.397(7)	N1-C14-C13	106.2(4)
C7-N1	1.467(6)	N2-C14-N1	121.9(5)
C14-N1	1.388(7)	N2-C14-C13	131.9(5)
C14-N2	1.295(7)	C1-N1-C7	119.3(4)
C15-N2	1.408(7)	C14-N1-C1	127.4(4)
		C14-N1-C7	111.8(4)
		C14-N2-C15	119.3(5)

Table S6: Crystallographic data and structure refinement for [6a][TFA]$_2$ H_2O	
Identification code	**[6a][TFA]$_2$**
Empirical formula	$C_{44}H_{34}F_6N_4O_5Re_2$
Formula weight	1185.15
Temperature/K	160(1)
Crystal system	monoclinic
Space group	C2/c
a/Å	15.32330(10)
b/Å	16.77620(10)
c/Å	15.10910(10)
α/°	90
β/°	101.2780(10)
γ/°	90
Volume/Å^3	3809.05(4)
Z	4
ρ_{calc}g/cm^3	2.067
μ/mm^{-1}	12.977
F(000)	2280.0
Crystal size/mm^3	0.14 × 0.11 × 0.08
Radiation	Cu Kα (λ = 1.54184)
2Θ range for data collection/°	7.898 to 148.99
Index ranges	-18 ≤ h ≤ 19, -20 ≤ k ≤ 20, -18 ≤ l ≤ 18
Reflections collected	39299
Independent reflections	3889 [R_{int} = 0.0233, R_{sigma} = 0.0090]
Data/restraints/parameters	3889/474/348
Goodness-of-fit on F^2	1.091
Final R indexes [I>=2σ (I)]	R_1 = 0.0355, wR_2 = 0.0909
Final R indexes [all data]	R_1 = 0.0356, wR_2 = 0.0910
Largest diff. peak/hole / e Å^{-3}	1.89/-1.63

Data of [**6b**][TFA]$_2$ 2(H_2O)

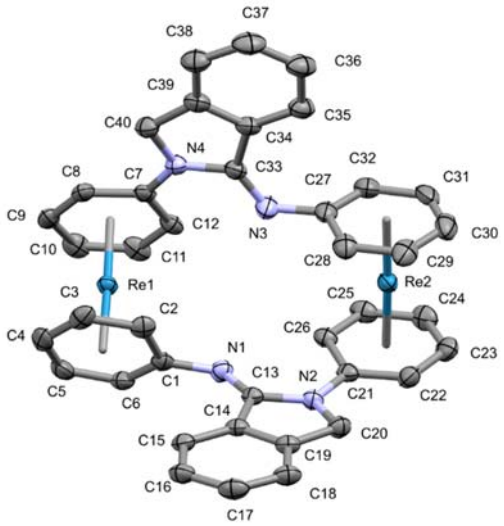

Figure S27: ORTEP representation of [**6b**]$^{2+}$. Ellipsoids represent 50% probability. Counter ions, solvent molecules and ydrogen atoms are omitted for clarity.

Table S7: Tabulated values of selected bond lengths and angles of the crystallographic data of **[6b]**[TFA]$_2$ 2(H_2O).

Selected bond lengths [Å]		Selected angles [°]	
Centroid-Re-Centroid	1.7346(16)/1.738(14) 1.7271(13)/1.7393(13)	Centroid-Re-Centroid	178.40(8)/177.96(8)
N1-C1	1.407(4)	C13-N1-C1	120.2(3)
N1-C13	1.281(4)	C13-N2-C20	112.0(3)
N2-C13	1.396(4)	C13-N2-C21	127.5(3)
N2-C20	1.467(4)	C21-N2-C20	119.6(3)
N2-C21	1.409(4)	C33-N3-C27	120.4(3)
N3-C27	1.402(5)	C7-N4-C40	120.6(3)
N3-C33	1.280(5)	C33-N4-C7	127.3(3)
N4-C7	1.400(4)	C33-N4-C40	112.0(3)
N4-C33	1.392(4)		
N4-C41	1.473(4)		

Table S8: Crystallographic data and structure refinement for $[6b][TFA]_2$ $2(H_2O)$	
Identification code	**$[6b][TFA]_2$**
Empirical formula	$C_{44}H_{36}F_6N_4O_6Re_2$
Formula weight	1203.17
Temperature/K	160(1)
Crystal system	monoclinic
Space group	$P2_1/c$
a/Å	20.9702(2)
b/Å	11.48170(10)
c/Å	16.73010(10)
α/°	90
β/°	101.4320(10)
γ/°	90
Volume/Å^3	3948.25(6)
Z	4
ρ_{calc}g/cm^3	2.024
μ/mm^{-1}	12.551
F(000)	2320.0
Crystal size/mm^3	0.09 × 0.05 × 0.02
Radiation	Cu Kα (λ = 1.54184)
2Θ range for data collection/°	8.604 to 148.944
Index ranges	-25 ≤ h ≤ 26, -13 ≤ k ≤ 14, -20 ≤ l ≤ 20
Reflections collected	41009
Independent reflections	8059 [R_{int} = 0.0272, R_{sigma} = 0.0202]
Data/restraints/parameters	8059/426/620
Goodness-of-fit on F^2	1.018
Final R indexes [I>=2σ (I)]	R_1 = 0.0240, wR_2 = 0.0587
Final R indexes [all data]	R_1 = 0.0263, wR_2 = 0.0597
Largest diff. peak/hole / e Å^{-3}	1.44/-1.27

3 Mechanistic Considerations of the Formation of [5]+, [6a]$^{2+}$ and [6b]$^{2+}$

Monitoring of the reaction progress from [**4**]$^{+}$ to the *ansa*-complex [**5**]$^{+}$ and the dinuclear species [**6a**]$^{2+}$ and [**6b**]$^{2+}$ was performed by analysis of an aliquot of the reaction mixtures *via* UPLC-MS. Consumption of the starting material as well as formation of new species, conversion of one intermediate to another and formation of the products, [**5**]$^{+}$, [**6a**]$^{2+}$ and [**6b**]$^{2+}$ were monitored. The results thus obtained are presented in Scheme S1 below. We propose the *ansa*-complex formation to proceed *via* imine formation (observed as [M + H_2O]$^{+}$, 507.05 m/z) rapidly followed by nucleophilic attack of the second amine onto the imine. Nucleophilic attack of the secondary amine onto the remaining aldehyde moiety efficiently produced the key intermediate **I**. Dehydration and [1,3] hydride shift induced by exocyclic imine formation completed the sequence and delivered [**5**]$^{+}$. R. Chebolu *et. al* published an insightful investigation into a similar mechanistic sequence for 1,2-disubstituted benzimidazoles involving a [1,3] hydride shift mentioned before upon which we base our proposal.[12]

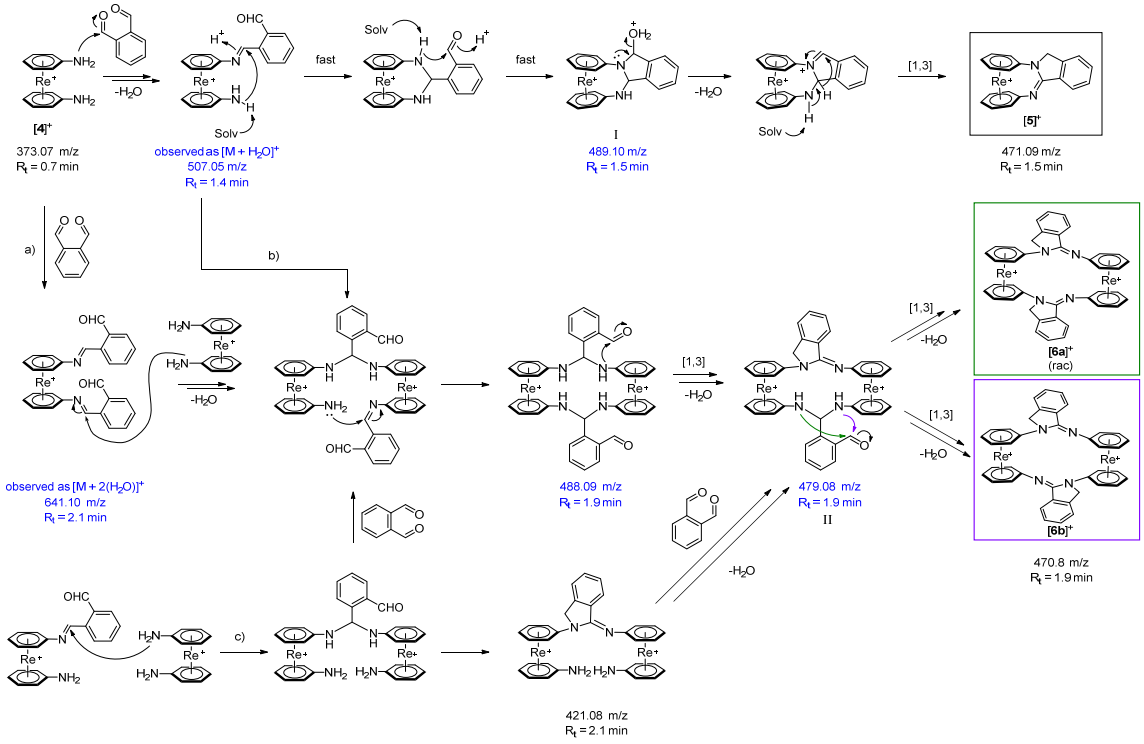

Scheme S1: Step-by-step mechanism of the formation of [**5**]$^{+}$ (top row) and an illustration of the pathways leading to the dinuclear species [**6a**]$^{2+}$ and **[6b]**$^{2+}$. Blue m/z values correspond to species observed with UPLC-ESI-MS while black represents isolated compounds.

Furthermore, we propose that [**6a**]$^{2+}$ and [**6b**]$^{2+}$ were formed through a combination of three different pathways: a) formation of an imine between [**4**]$^{+}$ and two OPA molecules, b) dimerization of two monoimines, and c) combination of one monoimine and [**4**]$^{+}$. All pathways ultimately proceeded *via* the key intermediate **II**, which we observed as [M]$^{2+}$ with 479.08 m/z (R_t = 1.9 min). Formation of [**6a**]$^{2+}$ and [**6b**]$^{2+}$ proceeded *via* nucleophilic attack of either one of the secondary amines present in II (blue and green pathways). Finally, a [1,3]

hydride shift completed the sequence and delivered the two dimeric macrocycles [**6a**]$^{2+}$ and [**6b**]$^{2+}$ respectively.

4 Coalescence Investigations of [6a]$^{2+}$

Temperature coalescence behavior was observed in the ^{1}H-NMR spectra of [**6a**][TFA]$_2$**.** We applied the methods described by Zimmer and coworkers to determine the activation energy (E_A) and activation energy barrier ($\Delta G^{\ddagger}$).[13] Therefore, ^{1}H-NMR spectra of [**6a**][TFA]**$_2$** were recorded at various temperatures. The experimental spectra of the CH_2 groups were (Figure **S28**, left row) were fitted with simulated spectra to determine exchange rates (k) at various temperatures. Simulations were performed using the DNMR3 function built in the open-source program SpinWorks 4.[14] The resulting spectra are depicted in Figure S28 below (right row).

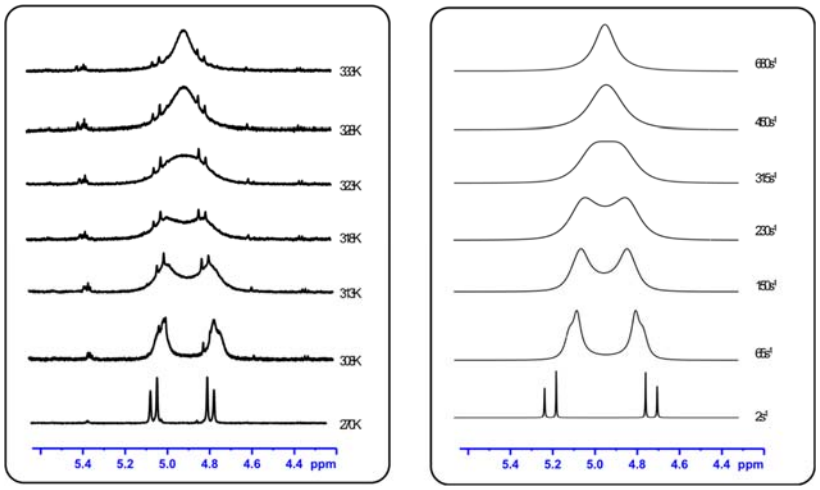

Figure S28: Experimental ^{1}H-NMR spectra of [**6a**]$^{2+}$ at various temperatures (left) and simulated spectra with the respective rates (right).

The rates determined through the simulated spectra were used to generate an Arrhenius plot (Figure S29) which allowed the determination of the activation energy (E_A) according to the following formula:

$$E_A = -(slope * R)$$

Using R = 8.3144 J*K^{-1}*mol^{-1}, the slope given by the linear regression and its corresponding error, the activation energy was calculated to be **E_A= 69.55±2.19 kJ·mol^{-1}**.

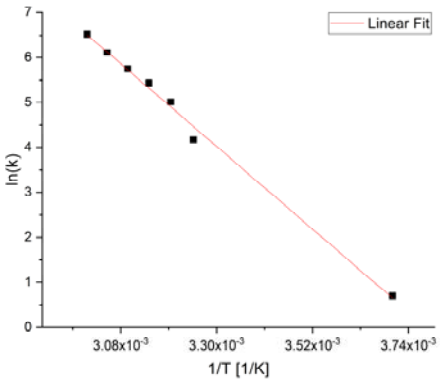

Figure S29: Arrhenius plot, ln(k) versus 1/T. Linear fit: r^2 = 0.99507, slope = -8364.82±263.21, y-intercept: 31.62±0.85.

Furthermore, activation energy barrier ($\Delta G^{\ddagger}$) of the equilibrium was determined based on the modified Eyring equation showed below:

$$\Delta G^{\ddagger} = RT * \left[23.760 + \ln\left(\frac{T}{k_r}\right)\right]$$

Table A1: Rates, calculated $\Delta G^{\ddagger}$ values and corresponding temperatures.

Temperature [K]	Rate [s^{-1}]	$\Delta G^{\ddagger}$ [kJ/mol]
270	2	64.350
308	65	64.829
313	150	63.747
318	230	63.678
323	315	63.876
328	450	63.934
333	680	63.807

Averaging the data above and calculating the standard deviation, we obtained an activation energy barrier of **$\Delta G^{\ddagger}$ = 64.03±0.41 kJ·mol^{-1}**. To check this data, we performed an Eyring plot (Figure S30)and obtained **$\Delta H^{\ddagger}$ = 67.07±2.17 kJ·mol^{-1}** form the slope (slope = $-\Delta H^{\ddagger}/R$) and **$\Delta S^{\ddagger}$ = 9.7±0.2 J·mol^{-1}** from the Y-intercept (intercept = $\Delta S^{\ddagger}/R$ + 23.76). Using **$\Delta G^{\ddagger} = \Delta H^{\ddagger} - T \cdot \Delta S^{\ddagger}$ = 64.03 kJ·mol^{-1}** we could nicely verify the calculations of the free activation energy barrier.

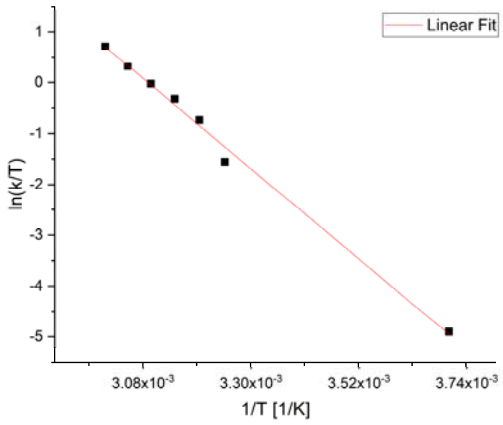

Figure S30: Eyring plot, ln(k/T) versus 1/T. linear fit: r^2 = 0.99475, slope = --8067.26±261.99, y-intercept: 24.93±0.84.

A closer look at the exchange process described above revealed that it involved only the racemate [**6a**][TFA]$_2$. We base this on the fact that temperature dependent signal broadening in the ^{1}H NMR was only observed for signals of [**6a**][TFA]$_2$. This exchange behavior was further investigated with 2D-ROESY correlation data (Figure S31). Spectra of a mixture of [**6a**][TFA]$_2$ and [**6b**][TFA]$_2$ were measured at 270K and the data showed no exchange signals between [**6a**][TFA]$_2$ and [**6b**][TFA]$_2$ but only of signals belonging to [**6a**][TFA]$_2$. We thus believe that the exchange process observed here originates from dynamic interchange of the *(P)*- and *(M)*-enantiomers of [**6a**][TFA]$_2$.

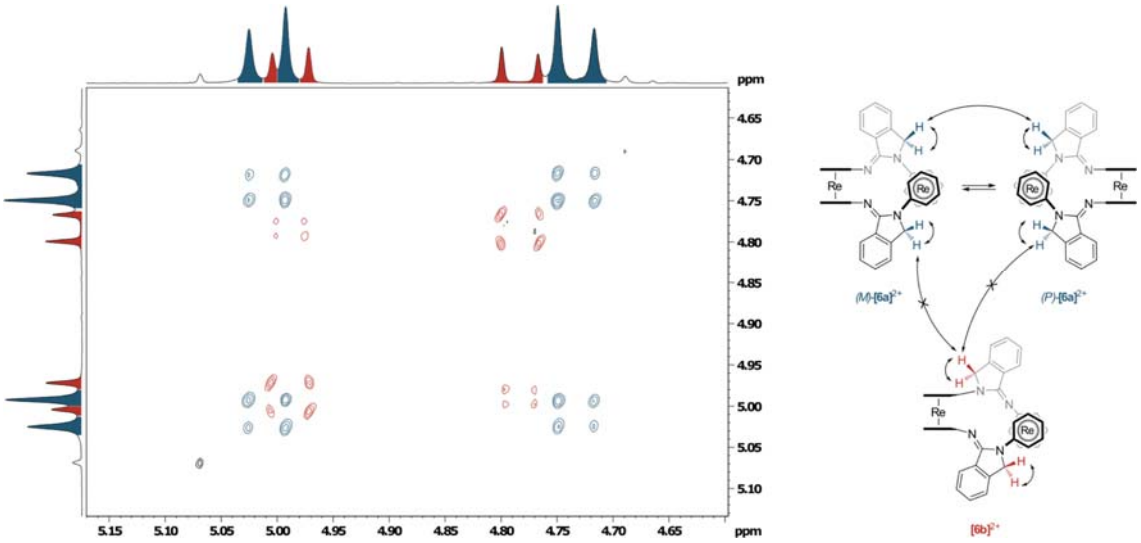

Figure S31: ROESY correlation spectra of a mixture of the racemate of [**6a**][TFA]$_2$ and [**6b**][TFA]$_2$ in a 2.75:1 molar ratio. Signals of [**6a**][TFA]$_2$ are color coded in blue, those of [**6b**][TFA]$_2$ in red.

5 UV/Vis Data

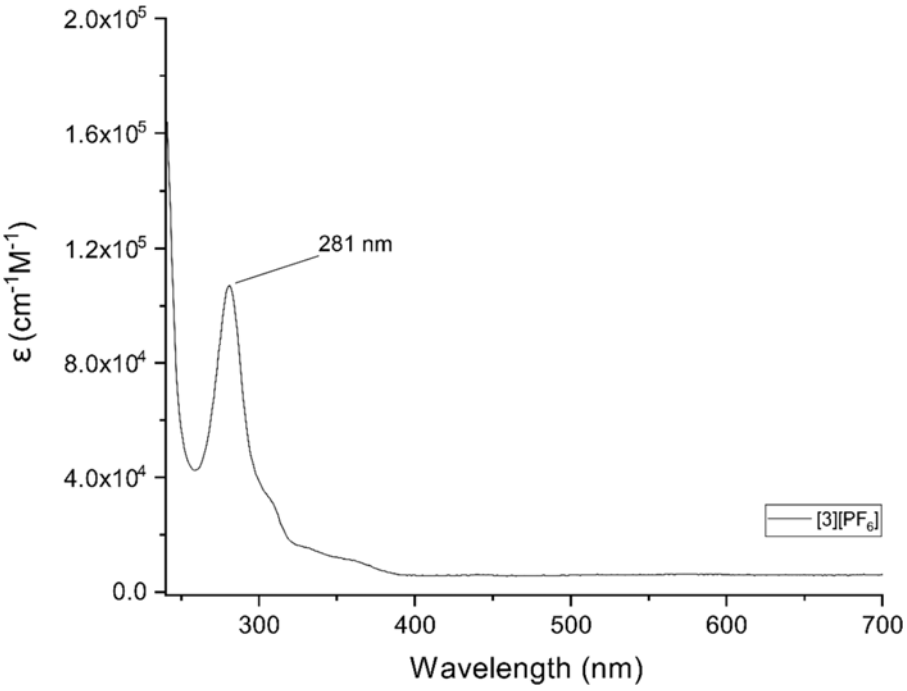

Figure S32: UV/Vis Spectrum of [**3**][PF_6] in CH_2Cl_2.

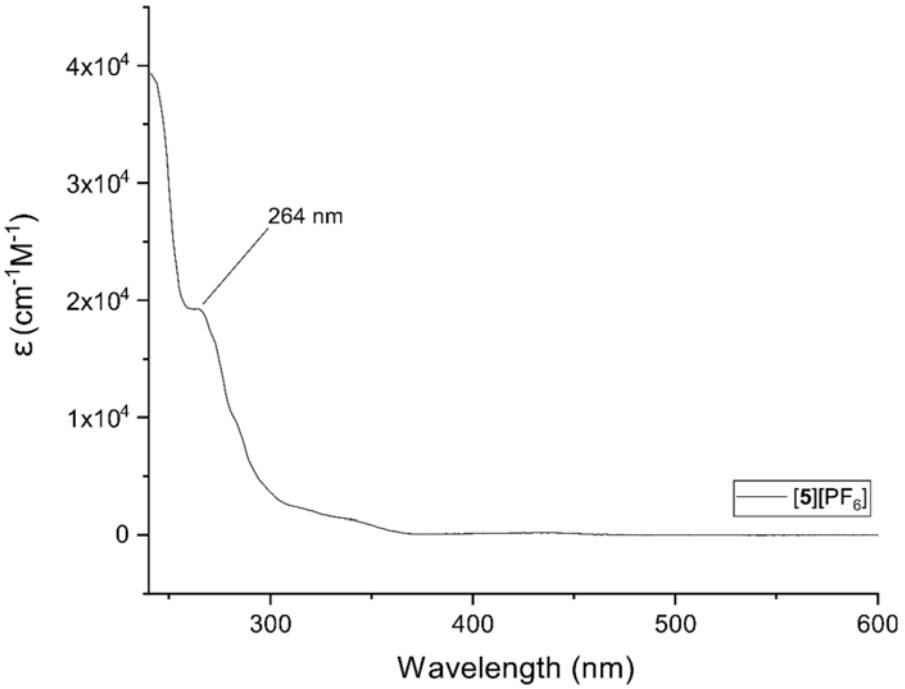

Figure S 33: UV/Vis Spectrum of [**3**][PF_6] in CH_2Cl_2.

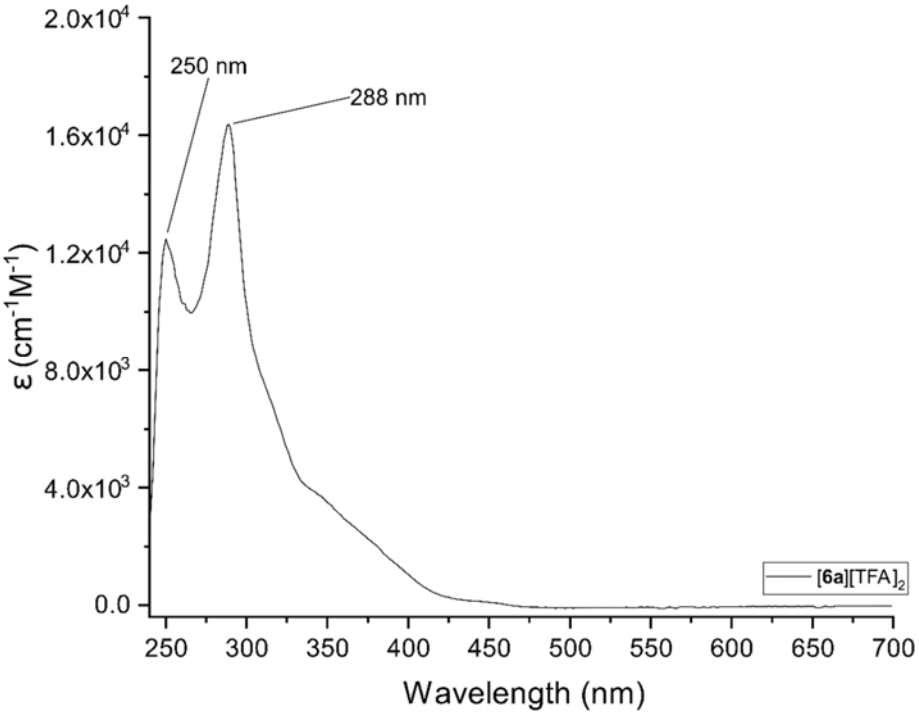

Figure S34: UV/Vis Spectrum of [**6a**][TFA]$_2$ in CH_2Cl_2.

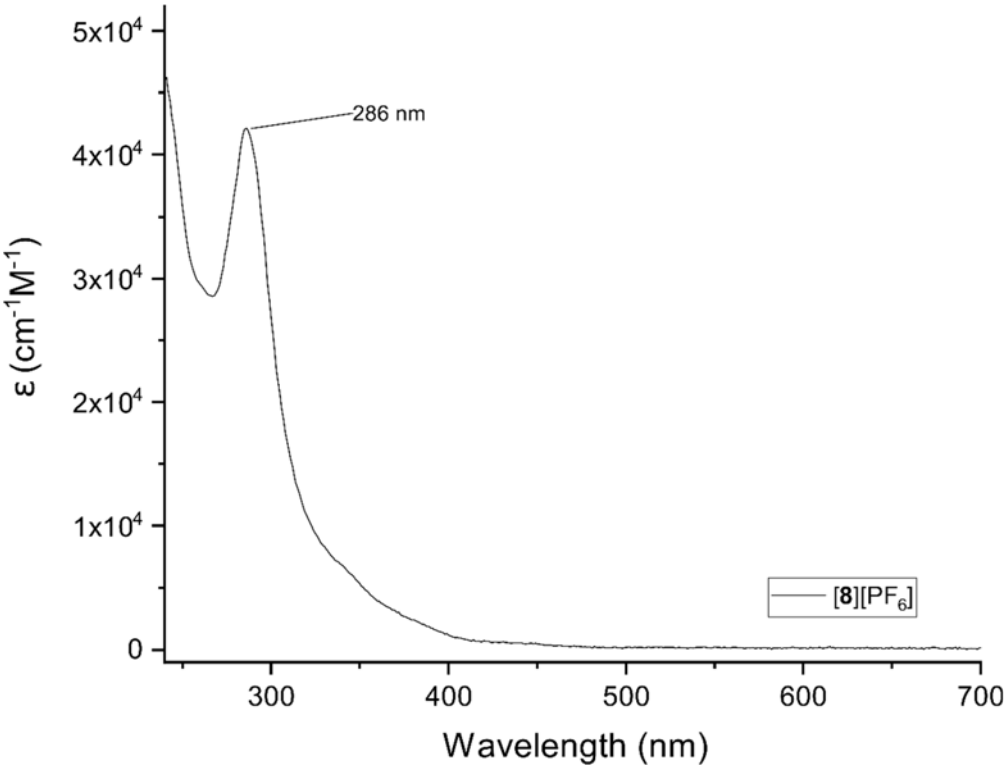

Figure S 35: UV/Vis Spectrum of [**8**][PF_6] in CH_2Cl_2.

6 References

1. R. C. Clark and J. S. Reid, *Acta Crystallogr. A*, 1995, **51**, 887-897.
2. CrysAlisPro (version 1.171.41.113a), Yarnton, Oxfordshire, England, 2019 – 2021.
3. O. V. Dolomanov, L. J. Bourhis, R. J. Gildea, J. A. K. Howard and H. Puschmann, *J. Appl. Crystallogr.*, 2009, **42**, 339-341.
4. G. Sheldrick, *Acta Crystallogr. A*, 2015, **71**, 3-8.
5. G. Sheldrick, *Acta Crystallogr. C*, 2015, **71**, 3-8.
6. A. Spek, *Acta Crystallogr. D*, 2009, **65**, 148-155.
7. E. A. Trifonova, D. S. Perekalin, K. A. Lyssenko and A. R. Kudinov, *J. Organomet. Chem.*, 2013, **727**, 60-63.
8. G. Meola, H. Braband, S. Jordi, T. Fox, O. Blacque, B. Spingler and R. Alberto, *Dalton Trans.*, 2017, **46**, 14631-14637.
9. D. Hernández-Valdés, F. Avignon, P. Müller, G. Meola, B. Probst, T. Fox, B. Spingler and R. Alberto, *Dalton Trans.*, 2020, **49**, 5250-5256.
10. G. Meola, H. Braband, P. Schmutz, M. Benz, B. Spingler and R. Alberto, *Inorg. Chem.*, 2016, **55**, 11131-11139.
11. Q. Nadeem, F. Battistin, O. Blacque and R. Alberto, *Chem. Eur. J.*, 2022, **28**, e202103566.
12. R. Chebolu, D. N. Kommi, D. Kumar, N. Bollineni and A. K. Chakraborti, *J. Org. Chem.*, 2012, **77**, 10158-10167.
13. K. D. Zimmer, R. Shoemaker and R. R. Ruminski, *Inorg. Chim. Acta*, 2006, **359**, 1478-1484.
14. SpinWorks (v 4.0.5.0) K. Marat, University of Manitoba, Winnipeg, Canada, 2014.